National Research Fund (FNR)

Luxembourg

Final Report

# DEVELOPING MATHEMATICAL MODELS, ALGORITHMS AND PROGRAMMING TOOLS FOR ANALYSIS OF ACTIN BASED MOTILITY

*FNR Fellow:*

*Dr.* Petr V. Nazarov

*Supervisor:*

*Prof.* Evelyne Friederich

*Co-Authors:*

Eugene Barsukov

Aliaksandr Halavatyi

Eugene Ivashkevich

*Dr.* Mikalai M. Yatskou

*Prof.* Vladimir V. Apanasovich

Minsk – Luxembourg, 2007

# CONTENTS

# ABBREVIATIONS

**Reagents**

| | |
|---|---|
| ACF | F-actin (any) |
| ACG | G-actin (any) |
| ACT | ActA |
| ADF | F-actin with ADP |
| ADG | G-actin with ADP |
| ARA | Arp2/3 complex, activated |
| ARF | Arp2/3 complex, bound |
| ARP | Arp2/3 complex, free |
| ATF | F-actin with ATP |
| ATG | G-actin with ATP |
| CAF | Capping protein, bound at barbed |
| CAP | Capping protein, free |
| COD | Cofilin-ADP-actin |
| COP | Cofilin free |
| CPF | Capping protein, bound at pointed |
| FDB | Barbed end with ADP-actin at the end |
| FDP | Pointed end with ADP-actin at the end |
| FIB | Barbed end (any) |
| FIP | Pointed end (any) |
| FOF | Formin in a bound form |
| FOP | Formin, free |
| FTB | Barbed end with ATP-actin at the end |
| FTB | Pointed end with ATP-actin at the end |
| PAD | Profilin-ADP-actin |
| PAT | Profilin-ATP-actin |
| PRO | Profilin |

**Reactions**

| | |
|---|---|
| ASDB | Association of ADP actin with barbed end |
| ASDP | Association of ADP actin with pointed end |
| ASSB | Association at barbed end |
| ASSP | Association at pointed end |
| ASTB | Association of ATP actin with barbed end |
| ASTF | Association of ATP actin with bared end with formin |
| ASTP | Association of ATP actin with pointed end |
| CAPB | Capping of barbed end |
| DEPO | Complete depolymerization of the short filaments |
| DISB | Dissociation at barbed end |
| DISP | Dissociation at pointed end |
| DSDB | Dissociation of ADP actin at barbed end |
| DSDP | Dissociation of ADP actin at pointed end |
| DSTB | Dissociation of ATP actin at barbed end |
| DSTP | Dissociation of ATP actin at pointed end |
| DTOT | Change from ADF TO ATF |
| FMNB | Association of formin with barbed end |
| FNUC | Nucleation by forming |
| SEVR | Severing reaction |
| SEVR | Severing of filament by ADF/cofilin |
| SNUC | Spontaneous nucleation |
| TESP | Capping of pointed end by testin |
| TTOD | Change from ATF TO ADF in filaments |

# 1. INTRODUCTION

Computational modeling is increasingly recognized as a crucial tool for making sense of the vast quantities of complex experimental data that are now being collected in biology. Over the last decade many mathematical quantitative and qualitative models at the level of biochemical reactions and regulatory networks have been developed. For example, the hybrid modeling approach was proposed that integrates conventional biochemical kinetic modeling within the framework of an electrical circuit simulation (McAdams and Shapiro, 1995). A structured model of gene expression, which incorporates the stochastic behavior of cellular processes, was developed to examine the "all-or-none" phenomenon observed in autocatalytic systems (Carrier and Keasling, 1999). The kinetics of prokaryotic gene expression has been modeled by the Monte Carlo computer simulation algorithm of Gillespie in the work of Kierzek et al (Kierzek et al., 2001). The models of cellular clocks, based on genetic networks with positive and negative regulatory elements are proposed in (Barkai and Leibler, 2000) and validated in  (Vilar et al., 2002), where it was demonstrated that under some conditions, this oscillator is not only resistant to but, paradoxically, also enhanced by the intrinsic biochemical noise. The effective algorithm for the stochastic simulation of systems composed of both intensive metabolic reactions and regulatory processes involving small numbers of molecules has been developed and applied to the simulation of glucose, lactose, and glycerol metabolism in Escherichia coli (Puchalka and Kierzek, 2004).

Different software tools are used for the practical computational modeling. A list of specialized software tools is available today to provide facilities for mathematical modeling and analysis of complex biological networks (Hucka et al., 2004). Among them the following software tools are widely used: Ingenuity (www.ingenuity.com), Ariadna Genomics (www.ariadnegenomics.com), GeneNetWorks (http://wwwmgs.bionet.nsc.ru), JDesigner (http://sbw.kgi.edu), CellDesigner (http://www.celldesigner.org). Many simulation algorithms realized in the above-mentioned tools and based on the existing formalisms.

This work is devoted to the developing of models and simulation-based formalism of data analysis to study the actin polymerization. Actin polymerization is a complex cell process (see the review by Pollard (Pollard and Borisy, 2003)), involved in cytoskeleton formation, cell movement and division. The study of this process, among pure scientific interest in understanding biophysical principles of cell motility, is motivated by the following practical reasons. Several pathogens, like *Listeria monocytogenes*, use actin polymerization for propulsion inside infected cells (Soo and Theriot, 2005). The motility of cancer cells and metastasis spread is significantly dependent on actin polymerization (Giganti and Friederich, 2003; Yamazaki et al., 2005). By influencing the actin polymerization process, in principle, it should be possible to prevent propulsion and fissiparity of pathogens and increase the activity of leukocytes, fibroblasts and neural cells.

Globular monomers of actin protein, G-actins (ACG) have the small tendency to aggregate with the rate constant $k_{SNUC}$ under the certain condition and form filamentous polymers with asymmetrical ends. The asymmetry of the ends reveals in different aggregation rate, therefore an actin filament grows faster at barbed end (FIB), then at another, pointed, end (FIP). The energy freed in actin aggregation is used by cells as a source of mechanical forces, which can be transferred into the cell propulsion. The process of actin assembly is influenced by the concentration of G-actins, physical conditions and, what is crucial, different regulative proteins: Arp 2/3 complexes (ARP), different capping proteins (CAP), ADC/cofilin (ACD), to name just a few (Pollard and Borisy, 2003). In our study we selected the most relevant proteins, usually used in laboratories for *in vitro* study of actin polymerization: actin, Arp2/3, ADC/cofilin, capping protein and profilin. Actin is directly involved in filament formation. Arp2/3, ADC/cofilin, capping proteins take part in filament branching, severing, and capping filament ends correspondingly. Profilin replaces ADP in the free G-actins, by ATP and so, charges them for further polymerization cycle.

Despite a big number of theoretical works related to actin polymerization, the formalism for the modeling of the processes in not completely developed. The existing analytical models are obtained for the special cases and preserve some natural limitations (however they are successfully used for to obtain bright results for these special cases). For instance the model for filament capping and branching of Carlsson (Carlsson, 2005; Carlsson et al., 2004) clarify the way of filament branching. In this works three models were considered and validated: barbed-end branching, side-branching and side branching with aging of F-actins (the last models showed best prediction). However, the strict quantitative correspondence between analytical predictions and experimental data for the system with capping and branching is questionable (see Fig. 7 in (Carlsson et al., 2004)). Most of analytical models were developed to estimate parameters in specific systems and cannot by used in a general case (see (Romero et al., 2004), etc). Moreover, the specificity of the developed analytical models significantly hampers their validation: the observed effect can be the real property of the studied system, as well as the result of a logical inaccuracy.

Therefore it is important to develop the computational simulation models, which can be used in a general case to predict the behavior of actin systems from the first principle. Although such models have been presented in some works, for instance (Alberts and Odell, 2004), (Carlsson, 2001), the lack of a systematic consideration of the simulation modeling of actin polymerization still exists. The model of Alberts and Odell (Alberts and Odell, 2004) has been developed mainly to study the mechanical properties of actin filament-bacteria interactions, and their paper does not contain the description of the simulation model for the related biochemical processes (polymerization, branching, capping). Therefore it is too approximate and rough to be used to study this processes in detail. The model presented by Carlsson (Carlsson, 2001) is based on a rather time-consuming simulation algorithm (which is by a factor of ~100 slower then the method used here),

and can be significantly enhanced using Gillespie's (Gillespie, 1977) and Gibson-Bruck (Gibson and Bruck, 2000) approaches.

Important and still open task is developing methodology for application of the simulation models directly for data analysis. This task is used in biophysics, when the studied systems and processes cannot be described analytically with satisfactory precision. In such a case computational simulation models can be used to fit the data as was described early (Nazarov et al., 2004; Nazarov et al., 2006; Yatskou et al., 2001).

Experiments aimed at the study of actin polymerization can be divided into two groups. The first group contains the experiments based on observation of mechanical results of the actin filament formation: bacteria (Brieher et al., 2004) or polysterol beads (Giganti et al., 2005) propulsion, actin-mediated force generation (Marcy et al., 2004). The experiments of the second group operate with pyrene-labeled actin, and obtain information from pyrene fluorescence, detected exclusively from labeled F-actin (Kouyama and Mihashi, 1981; Mahaffy and Pollard, 2006). Several sections of the work have been specifically aimed at these experiments. For example, the model and software tool has been developed for the fast analysis of the actin-pyrene experimental data. The mesoscale mechanical model – is an attempt to simulate bead propulsion in the actin assays. Although this kind of simulation is not applicable to the direct data analysis due to high computational costs, it can be used to check hypotheses, verify analytical models and plan experiments.

In the current work we also propose rather general formalism to simulation of actin polymerization, which, being realized as a software tool, should in principle allow to a biologist to build his own systems by fast and vivid combination of proposed reagents and interactions.

## 2. REVIEW OF THE PREVIOUS ACTIN-RELATED STUDIES

### *2.1. Biochemistry*

#### 2.1.1. Actin polymerization process at the reaction scale

Actin polymerization is a rather complex process, involving a number of protein components (see review by Pollard (Pollard and Borisy, 2003)). The main participants of the process are listed in the Table 1, and the model of the biochemical influences is given in Fig 1. Along with the standard "concentration" polymerization (mostly at barbed end), this process can be stimulated by formin, which interacts with barbed ends of filaments, speeding up polymerization; Arp2/3 complex able to nucleate new filaments, producing branching structures (Pollard and Beltzner, 2002); bundling proteins can decrease the speed of depolymerization, shifting equilibrium towards elongation of filaments (Loomis et al., 2003).

Table 1.1. Brief description of the participating proteins

| Protein | Description | References |
|---|---|---|
| actin | Main building block of actin-filament. Present in two forms G-actin (globular, monomer) and F-actin (filament, polymer). Actin usually is associated with a ATP/ADP molecules, forming 4 subsets of actin population (F-ATP, F-ADP, G-ATP, G-ADP) with different polymerization properties. | All mentioned below |
| profilin | Performs exchange G(ADP)-actin → G(ATP)-actin. | (Pollard and Borisy, 2003; Romero et al., 2004) |
| capping | Capping protein inhibits the polymerization by occupation of the free barbed ends of actin filaments | (Pollard and Borisy, 2003; Romero et al., 2004; Vignjevic et al., 2003) |
| formin | A group of proteins involved in the polymerization of actin. It cooperates in rapidly assembling profilin-actin into long filaments while remaining continuously associated with the fast-growing barbed end. | (Kovar, 2006; Romero et al., 2004) |
| Arp2/3 | Actin-Related Proteins Arp2/3 complex is a seven-subunit protein that serves as nucleation sites for new actin filaments. The complex binds to the sides of existing filaments and initiates growth of a new filament at a distinctive 70°. As a result of this nucleation of new filaments branched actin networks are created. | (Brieher et al., 2004; Giganti et al., 2005; Higgs and Pollard, 1999; Higgs and Pollard, 2001; Pollard and Beltzner, 2002; Sirotkin et al., 2005) |
| WASP (VCA) | WASP (Wiskott-Aldrich syndrome protein) activates Apr2/3. VCA is the active subunit of WASP. | (Bernheim-Groswasser et al., 2002; Carlier et al., 2003; Giganti et al., 2005; Higgs and Pollard, 1999; Higgs and Pollard, 2001; Loomis et al., 2003; Pollard and Borisy, 2003; Sirotkin et al., 2005; Vignjevic et al., 2003) |

| ActA | The protein of L. monocytogenes induces actin nucleation on the bacterial surface by activation of Arp2/3 and VASP (PRO domain). | (Carlier et al., 2003; DesMarais et al., 2005; Giganti et al., 2005; McGrath et al., 2000; Plastino et al., 2004; Pollard and Borisy, 2003) |
|---|---|---|
| VASP | This protein decreases branching of the filaments, at the same time increases the speed of L. monocytogenes and beads propulsion. The mechanism is not yet clear. The hypotheses are: VASP detach filaments from ActA complex, or compete with capping proteins | (Plastino et al., 2004; Samarin et al., 2003) |
| ADF/cofilin | ADF/cofilin is a family of actin-binding proteins that disassembles (severs) actin filaments | (Carlier et al., 2003; Pollard and Borisy, 2003) |
| fascin | Fascin is an actin-bundling protein and is thought to play a role in the formation of microfilament bundles of microspikes and stress fibers in cultured cells. | (Brieher et al., 2004; Plastino et al., 2004; Tseng et al., 2002; Vignjevic et al., 2003) |
| espin | Espin is an actin-bundling protein. | (Bartles et al., 1998; Loomis et al., 2003) |
| fimbrin | Fimbrin is an actin cross-linking protein. | (Giganti et al., 2005; Plastino et al., 2004) |
| T-plastin L-plastin | Actin cross-linking proteins | (Giganti et al., 2005; Janji et al., 2006) |
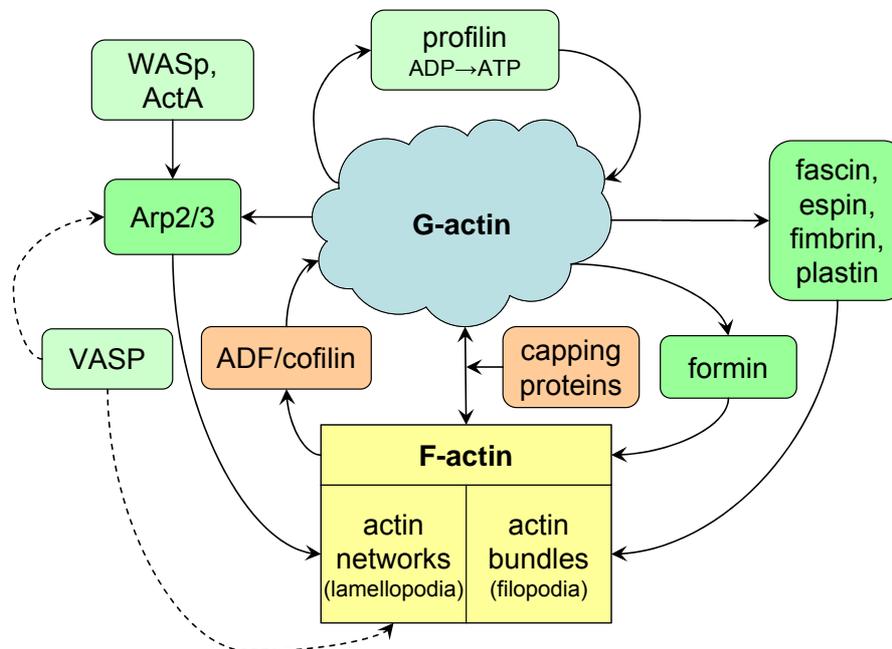


Figure 1.1. Schematic representation of a simplified biochemical network
related to the actin polymerization process

ADF/cofilin severs filaments. By its actin-severing activity, it creates new actin barbed ends for polymerization and also depolymerizes old actin filaments (Carlsson, 2006; DesMarais et al.,

2005). Capping proteins occupy barbed ends, thus preventing polymerization and shifting equilibrium towards depolymerization.

### 2.1.2. Reaction rates

The experimentally obtained rates for the actin-related reactions can be found in many papers. This information have been summarized and combined in one table.

Table 1.2. Reaction speeds

| Reaction | Value | Units | Reference |
|---|---|---|---|
| **_Nucleation_** | | | |
| Spontaneous nucleation<br>3 ACG $\rightarrow$ 3 ACF + FIB + FIP | $2.3 \times 10^{-11}$ | $\mu M^{-2} s^{-1}$ | (Samarin et al., 2003) |
| Spontaneous nucleation<br>3 ACG $\rightarrow$ 3 ACF + FIB + FIP | $1.05 \times 10^{-9}$ | $\mu M^{-2} s^{-1}$ | (Carlsson et al., 2004) |
| Capping protein –induced nucleation<br>CAP + 6ACG $\rightarrow$ FIP + CAF + 6 ACF | $2.9 \times 10^{-5}$ | $\mu M^{-6} s^{-1}$ | (Carlsson et al., 2004) |
| Arp2/3 –induced nucleation<br>ARP + 2ACG $\rightarrow$ ARF + 2ACG | $6.8 \times 10^{-6}$<br>$8.7 \times 10^{-5}$ | $\mu M^{-2} s^{-1}$ | (Carlsson et al., 2004) |
| **_Barbed end actin-filament reactions_** | | | |
| Association ATP-actin at barbed end<br>FIB + ATG $\rightarrow$ FIB + ATF | 11.5 | $\mu M^{-1} s^{-1}$ | (Pollard, 1986)<br>cited at (Alberts and Odell, 2004) |
| Dissociation of ATP-actin from barbed end<br>FTB $\rightarrow$ FIB + ATG | 1.4 | $s^{-1}$ | (Pollard, 1986)<br>c. at (Alberts and Odell, 2004) |
| Association ADP-actin at barbed end<br>FIB + ADG $\rightarrow$ FIB + ADF | 3.8 | $\mu M^{-1} s^{-1}$ | (Pollard, 1986)<br>c. at (Alberts and Odell, 2004) |
| Dissociation of ADP-actin from barbed end<br>FDB $\rightarrow$ FIB + ADG | 7.2 | $s^{-1}$ | (Pollard, 1986)<br>c. at (Alberts and Odell, 2004) |
| Barbed end association<br>FIB + ACG $\rightarrow$ FIB + ACF | 8.7 | $\mu M^{-1} s^{-1}$ | c. at (Carlsson et al., 2004) |
| Formin-enhanced barbed end grow<br>FOF+ACG $\rightarrow$ FOF + ACF | 110 | $\mu M^{-1} s^{-1}$ | (Romero et al., 2004) |
| **_Pointed  end actin-filament reactions_** | | | |
| Association ATP-actin at pointed end<br>FIP + ATG $\rightarrow$ FIP + ATF | 1.3 | $\mu M^{-1} s^{-1}$ | (Pollard, 1986)<br>c. at (Alberts and Odell, 2004) |
| Dissociation of ATP-actin from pointed end<br>FTP $\rightarrow$ FIP + ATG | 0.8 | $s^{-1}$ | (Pollard, 1986)<br>c. at (Alberts and Odell, 2004) |
| Association ADP-actin at pointed end<br>FIP + ADG $\rightarrow$ FIP + ADF | 0.16 | $\mu M^{-1} s^{-1}$ | (Pollard, 1986)<br>c. at (Alberts and Odell, 2004) |

| | | | |
|---|---|---|---|
| Dissociation of ADP-actin from pointed end<br>FDP → FIP + ADG | 0.27 | $s^{-1}$ | (Pollard, 1986)<br>c. at (Alberts and Odell, 2004) |
| Pointed end association<br>FIP + ACG → FIP + ACF | 1.3 | $\mu M^{-1}s^{-1}$ | c. at (Carlsson et al., 2004) |

<div align="center"><em>Capping</em></div>

| | | | |
|---|---|---|---|
| Barbed end capping 1<br>FIB + CAP → CAF | 3.0 | $\mu M^{-1}s^{-1}$ | (Schafer et al., 1996)<br>c. at (Alberts and Odell, 2004) |
| Barbed end uncapping 1<br>CAF → FIB + CAP | $4.0 \times 10^{-4}$ | $s^{-1}$ | (Schafer et al., 1996)<br>c. at (Alberts and Odell, 2004) |
| Barbed end capping 2<br>FIB + CAP → CAF | 8.0 | $\mu M^{-1}s^{-1}$ | (Carlsson et al., 2004) |
| Barbed end uncapping 2<br>CAF → FIB + CAP | 4.2 | $s^{-1}$ | (Carlsson et al., 2004) |
| Pointed end capping<br>FIP + CAP → CPF | ~ 1<br>~0.25 | $\mu M^{-1}s^{-1}$ | (Carlsson et al., 2004) |

<div align="center"><em>Hydrolysis</em></div>

| | | | |
|---|---|---|---|
| Hydrolysis stage 1 (vectorial model)<br>ATP → ADP-Pi | 12.3 | $s^{-1}$ | (Carlier et al., 1987)<br>c. at (Alberts and Odell, 2004) |
| Hydrolysis stage 2 (vectorial model)<br>ADP-Pi → ADP | 0.0026 | $s^{-1}$ | (Melki et al., 1996)<br>c. at (Alberts and Odell, 2004) |
| Aging of filamentous actins<br>ATF → ADF | 0.0087<br>0.0059 | $s^{-1}$ | (Carlsson et al., 2004) |
| Hydrolysis (by Carlier)<br>ATF → ADF | 60 | $s^{-1}$ | (Romero et al., 2004) |
| Formin-initiated hydrolysis<br>FOP (+ATF) → FOP (+ADF) | 340 | $s^{-1}$ | (Romero et al., 2004) |

<div align="center"><em>Branching</em></div>

| | | | |
|---|---|---|---|
| Arp2/3 activation<br>ACT + ARP → ARA (+ ACT ?) | 0.07 | $\mu M^{-1}s^{-1}$ | (Alberts and Odell, 2004) |
| Arp2/3 – ActA unbinding (deactivation?)<br>ARA → ARP (+ ACT ?) | 3.0 | $s^{-1}$ | (Alberts and Odell, 2004) |
| Active Arp2/3 binding<br>ARA + ACG → ARF + ACF (+ ACT ?) | 0.4 | $\mu M^{-1}s^{-1}$ | (Alberts and Odell, 2004) |
| Inverse reaction for Active Arp2/3 binding<br>???? | 30.0 | $s^{-1}$ | (Alberts and Odell, 2004) |
| Branching at end<br>ARA + FIB + 2ACG → ARF + 2FIB + 2ACF | ~0.43<br>~0.01 | $\mu M^{-3}s^{-1}$ | (Carlsson et al., 2004) |
| Branching at side<br>ARA + ACF + 2ACG → ARF + FIB + 3ACF | $\sim 1.4 \times 10^{-3}$<br>$\sim 4.9 \times 10^{-4}$ | $\mu M^{-3}s^{-1}$ | (Carlsson et al., 2004) |

| Actin recharge (ATP-ADP) | | | |
|---|---|---|---|
| Profilin replaces cofilin in COD complex COD (+PRO) → PAD (+COP) | 2 | $s^{-1}$ | (Mogilner and Edelstein-Keshet, 2002) |
| Cofilin replaces profilin in PAD complex PAD (+COP) → COD (+PRO) | 10 | $s^{-1}$ | (Mogilner and Edelstein-Keshet, 2002) |
| Profilin-initiated actin recharge PAD → PAT | 20 | $s^{-1}$ | (Mogilner and Edelstein-Keshet, 2002) |
| Severing | | | |
| Severing rate (assumption), in 1/μm ACF → ACG + FIB + FIP | 0.5 | $\mu m^{-1}s^{-1}$ | (Mogilner and Edelstein-Keshet, 2002) |
| Severing ACF → ACG + FIB +FIP | $2.3 \cdot 10^{-6}$ | $s^{-1}$ | (Carlsson, 2006) |

## 2.2. Biophysical experiments

Larger beads (up to 2 μm in diameter) can initiate movement only if surface asymmetry is introduced by coating the beads on one hemisphere. This explains why the relatively large *L. monocytogenes* requires polar distribution of ActA on its surface to move.

In the paper (Noireaux et al., 2000) authors studied similarities and differences in behavior of ActA coated beads and *L. monocytogenes* On ActA-grafted beads F-actin is formed in a spherical manner, whereas on the bacteria a "comet-like" tail of F-actin is produced. They show experimentally that the stationary thickness of the gel depends on the radius of the beads. Moreover, the actin gel is not formed if the ActA surface density is too low. A theoretical model able to explain how the mechanical stress (due to spherical geometry) limits the growth of the actin gel was proposed. The model predicts conditions for developing of actin comet tails.

In (Bernheim-Groswasser et al., 2002) was found that Wiskott Aldrich syndrome protein (WASP) subdomain, known as VCA, is sufficient to induce actin polymerization and movement when grafted on microspheres. Changes in the surface density of VCA protein or in the microsphere diameter markedly affect the velocity regime, shifting from a continuous to a jerky movement resembling that of the mutated 'hopping' *L. monocytogenes*.

A minimum motility medium containing five pure proteins (actin, Arp2/3, ADF/cofilin, profilin, capping proteins) was used in (Carlier et al., 2003) to study the motility of particles of various sizes and geometries (rods, microspheres).

Similar work is performed in (Cameron et al., 2004), where they have systematically varied a series of biophysical parameters and examined their effects on initiation of motility (of beads or *L. monocytogenes*), particle speed, speed variability, and path trajectory. Symmetry breaking and movement initiation occurred by two distinct modes: either stochastic amplification of local

variation for small beads in concentrated extracts, or gradual accumulation of strain in the actin gel for large beads in dilute extracts. Neither mode was sufficient to enable spherical particles to break symmetry in the cytoplasm of living cells.

Interesting experimental study in (Giardini et al., 2003) involved lipid vesicles covered with ActA in cytoplasmic extract, provides direct insight on the forces affecting vesicle surface due to analysis of its deformation. There was a spatial segregation of the pushing and retarding forces, such that pushing predominates along the sides of the vesicle, although retarding forces predominate at the rear. They estimated that the total net (pushing minus retarding) force generated by the actin comet tail is ~0.4–4 nN.

Similar system was used in (Upadhyaya et al., 2003), where they introduced an experimental system in which lipid vesicles coated with the *L. monocytogenes* virulence factor ActA are propelled by actin polymerization. The polymerization forces cause significant deformations of the vesicle. These deformations were used to obtain a spatially resolved measure of the forces exerted on the membrane using a model. Their results indicate that actin exerts retractile or propulsive forces depending on the local membrane curvature and that the membrane is strongly bound to the actin gel.

The work of Samarin et al (Samarin et al., 2003) is devoted to study the influences of VASP protein on the bead movement in a minimum motility medium. VASP increases branch spacing of filaments in the actin tail. The effect of VASP on branch spacing is opposed to the effect of capping proteins, however, VASP does not compete with capping proteins for binding barbed ends of actin filaments. VASP increases the rate of dissociation of the branch junction from immobilized ActA, which is the rate-limiting step in the catalytic cycle of site-directed filament branching.

VASP effects have been studied also in (Plastino et al., 2004). They show that the degree of filament alignment in the actin comet tails depended on the surface ratio of VASP to Arp2/3 activating proteins (PRO and VCA respectively). Alignment of actin filaments parallel to the direction of bead movement in the presence of VASP was accompanied by an abrupt 7-fold increase in velocity that was independent of bead size and by hollowing out of the comets. The actin filament-bundling proteins fimbrin and fascin did not appear to play a role in this transformation.

Giganti et al (Giganti et al., 2005) analyzes the effects of T-plastin/T-fimbrin. T-Plastin increased the velocity of VCA beads 1.5 times, stabilized actin comets and concomitantly displaced cofilin, an actin-depolymerizing protein. T-Plastin also decreased the F-actin disassembly rate and inhibited cofilin-mediated depolymerization. The bead speed, being a function of T-plastin concentration has a maximum around 1μM.

Considering beads in minimal biomimetic system (van der Gucht et al., 2005) shows that the symmetry breaking is based on the release of elastic energy. The dynamics of this process and the

thickness at which it occurs depend on the growth rate and mechanical properties of the actin gel. They explain experimental results with a model based on elasticity theory and fracture mechanics.

(Loomis et al., 2003) is devoted to study actin bundling by espin protein in vivo and in vitro. Espin crosslinks cause pronounced barbed-end elongation and, thereby, make a longer bundle without joining shorter modules.

The filament bundle formation form branched actin network is studied in (Vignjevic et al., 2003). They show that directions of filament barbed end in bundles and branched structures are opposite. They proposed a model for filopodial formation in which actin filaments of a preexisting branched network are elongated by inhibition of capping and subsequently cross-linked into bundles by fascin.

The group of Mitchison demonstrates in (Brieher et al., 2004) that *L. monocytogenes* motility can be separated into an Arp2/3-dependent nucleation phase and an Arp2/3-independent elongation phase. Elongation-based propulsion requires a unique set of biochemical factors, like fascin. The elongation-based reaction generates a hollow cylinder of parallel bundles that attach along the sides of the bacterium. Bacteria move faster in the elongation reaction than in the presence of Arp2/3, and the rate is limited by the concentration of G-actin.

F-actin gels of increasing concentrations (25–300 mM) display in vitro a progressive onset of birefringence due to orientational ordering of actin filaments as reported in (Helfer et al., 2005).

The work of Romero et al (Romero et al., 2004) is devoted to formins – initiators of actin assembly. They demonstrated that the forming's domains accelerates hydrolysis of ATP coupled to profilin-actin polymerization and uses the derived free energy for processive polymerization, increasing 15-fold the rate constant for profilin-actin association to barbed ends. Transitory formin-associated processes are generated by poisoning of the processive cycle by barbed-end capping proteins.

In original work by Marcy (Marcy et al., 2004) the forces generated during actin-based propulsion are directly measurement by micromanipulation. By pulling the actin tail away from the bead at high speed, they estimated the elastic modulus of the gel and measured the force necessary to detach the tail from the bead. By applying a constant force in the range of ~1.7 to 4.3 nN, the force-velocity relation was established.

Experimental results given in (Zicha et al., 2003) (FLAP) suggest the active transport G-actins to barbed ends of growing actin filament network.

### *2.3. Models*

#### 2.3.1. Models for biochemical processes

The mathematical models for the length distributions of actin filaments under the effects of polymerization/depolymerization, and fragmentation are given in (Edelstein-Keshet and Ermentrout, 1998; Ermentrout and Edelstein-Keshet, 1998).

Sept et al in (Sept and McCammon, 2001) provides information about computer simulations and free energy calculations, aimed to determine the thermodynamics and kinetics of actin nucleation and thus identify a probable nucleation pathway and critical nucleus size. The association kinetics for the formation of each structure are determined through a series of Brownian dynamics simulations. The results indicate that the trimer is the size of the critical nucleus.

Carlsson (Carlsson, 2006) have studied the effects of filament severing on their growth. From one side, the severing of the filaments leads to their dissociation, at the same time it increases the number of barbed ends (and therefore – growth speed). Severing and branching are found to act synergistically.

The model, based on the dendritic-nucleation hypothesis for lamellipodial protrusion is given in (Mogilner and Edelstein-Keshet, 2002). They consider a set of partial differential equations for diffusion and reactions of sequestered actin complexes, nucleation, and growth by polymerization of barbed ends of actin filaments, as well as capping and depolymerization of the filaments. The mechanical aspect of protrusion is based on an elastic polymerization ratchet mechanism. See also later works of Mogliner (Mogilner and Oster, 2003; Mogilner and Rubinstein, 2005).

#### 2.3.2. Mechanical models

In (van Oudenaarden and Theriot, 1999), the bead movement is considered. They show that small beads coated uniformly with a protein that catalyses actin polymerization are initially surrounded by symmetrical clouds of actin filaments. This symmetry is broken spontaneously, after which the beads undergo directional motion. They developed a stochastic theory, in which each actin filament is modeled as an elastic Brownian ratchet.

The process of actin gel formation around beads is also studied in (Noireaux et al., 2000). They propose a theoretical model to explain how the mechanical stress (due to spherical geometry) limits the growth of the actin gel. They deduced from the work that the force exerted by the actin gel on the bacteria is of the order of 10 pN.

The mechanical model taking into account pushing and back-drawing forces due to actin polymerization around *L. monocytogenes* is presented in (Gerbal et al., 2000). The model leads to a natural competition between growth from the sides and growth from the back of the bacterium, with

different velocities and strengths for each. This competition can lead to the periodic motion observed in a *L. monocytogenes* mutant.

The review by (Tracqui et al., 2004) contains information about different modeling approaches (mechanical models, differential equations, computational simulations). The review contains also information about the cytoskeleton computational simulation.

Simulation of single actin filaments is considered in (Ming et al., 2003). Model provides a theoretical basis set for a description of spontaneously occurring thermal deformations, such as undulations, of the filaments. The computationally synthesized deformational modes, in the very low-frequency regime, are in good agreement with theoretical solutions for long homogeneous elastic rods, which confirmed the usefulness of substructure synthesis method.

Nice works of Mogliner et al (Mogilner and Oster, 2003) and (Mogilner and Rubinstein, 2005) are devoted to theoretical study of lamellipodia and filopodia formation. In (Mogilner and Oster, 2003) they apply "tethered ratchet" model to derive the force-velocity relation for *L. monocytogenes* and discuss relations of their theoretical predictions to experimental measurements. In (Mogilner and Rubinstein, 2005) filament bundling and filopodia propulsion is modeled. The model explains characteristic interfilopodial distance of a few microns as a balance of initiation, lateral drift, and merging of the filopodia. The theory suggests that F-actin barbed ends have to be focused and protected from capping (the capping rate has to decrease one order of magnitude) once every hundred seconds per micron of the leading edge to initiate the observed number of filopodia.

The model for filopodia propulsion and filament aggregation is given in (Atilgan et al., 2006) . They find that a critical number of filaments are needed to generate net filopodial growth. Without external influences, the filopodium can extend indefinitely up to the buckling length of the F-actin bundle. Filopodia also attract each other through distortions of the membrane. Monte Carlo and analytical approaches have been used.

The model of deformation of ActA-covered vesicles is given in (Upadhyaya et al., 2003). They have used these deformations to obtain a spatially resolved measure of the forces exerted on the membrane using a model based on the competition between osmotic pressure and membrane stretching. The results indicate that actin exerts retractile or propulsive forces depending on the local membrane curvature and that the membrane is strongly bound to the actin gel.

### 2.3.3.  Computer simulation models

Alberts et al (Alberts and Odell, 2004) have been developed a holistic computational model for simulation of *L. monocytogenes* propulsion. They simulated actin polymerization at molecular level and take into account interactions of several types (rigidity, elasticity, Brownian) to simulate microeffects, which filaments has on a bacterium. The model which will be developed in our

project will be based on their approach (see section Proposed model), with several modification and enhancements.

Simulation presented in (Berro and Martiel, 2005) gives an idea how to handle concentration gradient. The simulation space was divided into cells with constant concentration and Gillespie algorithm was used to simulate reactions of actin polymerization inside those cells. The simulation was performed in 2D space.

## 3. MODELS AND METHODS

### 3.1. Proposed approaches and models hierarchy

#### 3.1.1. Simulation-based fitting approach to data analysis

The tasks, to be solved by a researcher when studying complex systems can be roughly divided into two groups: direct and inverse tasks.

**Direct application.** The prediction of the behavior of a system based on a known internal state and under different external conditions can be called the direct application of the simulation. To predict the system behavior, one has to build up the adequate model for the relevant processes in the system, and run the simulation taking into account the important initial conditions of the system and external influences. Stochastic and chaotic systems can be characterized in this way by statistical parameters obtained from simulations (therefore a number of independent simulation runs are essential). The comparison of the simulated end experimental behavior of the system suggests whether the initial model approximation was correct.

**Inverse application.** To solve the inverse task, means to find the hidden internal parameters of the system, or to define the structural model of a system by using external observations of the system behavior (experimental data).

**Simulation-based fitting** approach to data analysis was developed for the determination of physical parameters of complex systems, which cannot by described by analytical equations. The idea of simulation-based analysis is the approximation of experimental data by synthetic data obtained *via* simulation modeling. In comparison to standard analytical data fitting techniques, simulation-based analysis has the advantage that it provides information about natural physical and chemical parameters of the system and gives a direct insight in how they affect the experimental characteristics of the system (Yatskou et al., 2001). The general scheme of the inverse task solution by simulation modeling is given in Fig. 3.1. (Nazarov et al., 2004; Nazarov et al., 2006; Yatskou et al., 2001).

For an experimental object (block 1) using theoretical investigation approaches (block 2) the simulation model (block 3) is built. Then a number of experiments is performed on the object (block 4) which results in a set of experimental data, block 6 (for instance – fluorescence spectra). The researcher knows the experimental conditions and this gives additional knowledge about the properties of the object (temperature, pH, viscosity, etc) – block 5. Using the known parameters of the object and making assumptions about the sought parameters (block 10), the researcher runs the simulation modeling and obtains simulated data (block 8) in this numerical procedure (block 7). Comparing simulated data and experimental ones (by calculation of the error function), the optimization procedure (block 9) changes the estimation of the sought parameters, and the

algorithm cyclically goes to the numerical calculation again. This iterative search provides an estimation of the experimental parameters. If the model is adequate, and the inverse task is correctly formulated, the estimation found can be considered as a valid one.
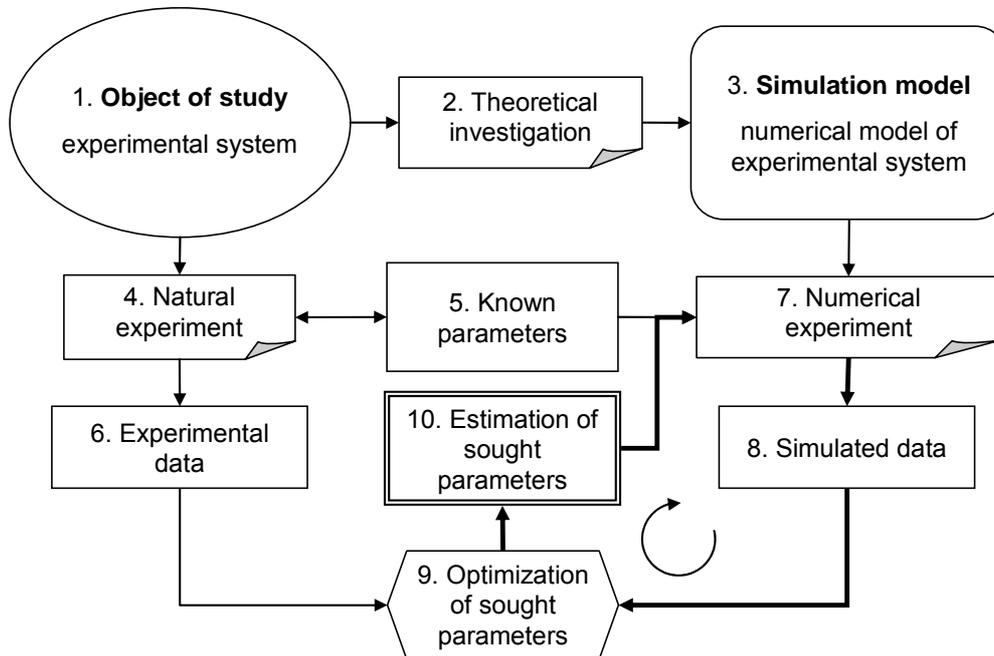


Figure 3.1. General solution of an inverse problem by the simulation-based fitting approach. Thick lines show the loop of the iterative estimation of the parameters sought.

### 3.1.2. Models hierarchy

To be able to simulate bead and bacteria propulsion it was decided to imitate the small volume of 3D-space filled with solution of proteins, filaments and small physical bodies. This mesoscale model is base on two main blocks (see Fig. 3.2): the model for molecular reactions and forces, representing mechanical interactions. In this model filaments and a bead (bacterium) are considered as physical objects, described by their coordinates, masses, velocities, inertia tensors, etc. Free proteins are considered in terms of concentrations. For the moment it was decided to assume constant protein concentrations in the considered volume. In future the volume can be divided into smaller sub-volumes and the gradients of concentrations could be taken into account.
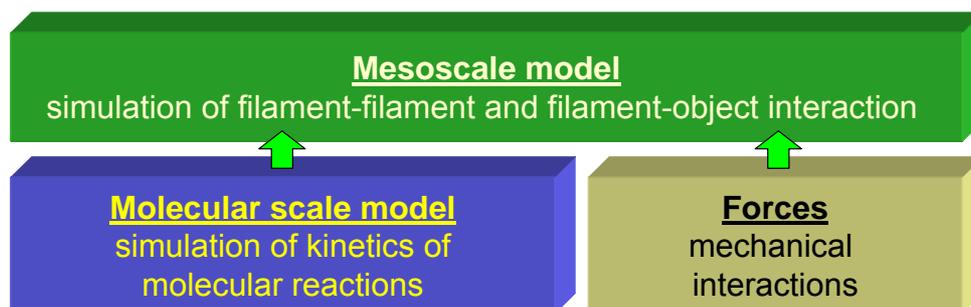


Figure 3.2. Hierarchy of the mesoscale model.

### 3.2. Analytical models for biochemical reactions

#### 3.2.1. Analytical model for the simplest case of actin polymerization

Consider first the simplest model for actin polymerization which can be described by 3 reactions: filament nucleation, association (consider net association at both pointed and barbed ends) and dissociation (net). As an additional reaction the complete destruction of the short filaments due to dissociation should be considered. Using the notification given in the Abbreviations section the considered reagents will be: G-actins (ACG), F-actins (ACF), and filament barbed ends (FIB). See below the reactions.

Nucleation:   $3ACG \rightarrow 3ACF + FIB$

Associations:  $FIB + ACG \rightarrow FIB + ACF$

Dissociation:  $FIB \rightarrow FIB + ACG \ (-ACF)$
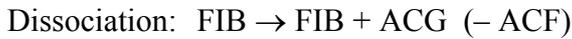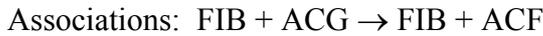
If the size of filament is less then 3 actin the dissociation reaction will lead to the filament destruction:           $FIB \rightarrow 3ACG \ (-3ACF)$.

This reactions can be described by a system of differential equation:

$$
\begin{cases}
\dfrac{d(FIB)}{dt} = k_{SNUC} \cdot ACG^3 - p_3 \cdot k_{DISB} \cdot FIB \\[2mm]
\dfrac{d(ACF)}{dt} = 3k_{SNUC} \cdot ACG^3 + k_{ASSB} \cdot FIB \cdot ACG - k_{DISB} \cdot FIB \cdot (1 + 2p_3)
\end{cases}
\tag{3.1}
$$

where $p_3$ is the probability to find a filament with length of 3 actins (minimal allowed value for the filament). Therefore $p_3 \cdot FIB$ defines the concentration of such filament in the solution. The expression for the parameter $p_3$ was empirically determined using the simulation model (see section 3.3) in the following form:

$$
p_3 \approx k_{SNUC} \cdot ACG^3 + 2 \frac{\sqrt{k_{DISB}}}{k_{ASSB}} \cdot \frac{FIB}{ACF}.
\tag{3.2}
$$

The first item of the Eq. 3.2 corresponds to the newly nucleated filaments, and the second is in inverse proportion to the average filament length $<l> = ACF/FIB$.

#### 3.2.2. Analytical model for the actin polymerization: branching, capping and severing

**Model overview.** To work out the simulation strategy and test the algorithms it was decided to simplify the considered molecular system (at this initial stage). This simplification significantly reduces the number of reactions; however, it saves all important features of the actin system: (de)polymerization, capping, branching and severing.

The simplifications are introduced by the following assumptions:

−   no difference between ATP- and ADP-carrying actins in filament;

−   very fast work of profilin (all ADP immediately are replaced by ATP) ;

- simplified nucleation reaction (3 G-actins can give a birth to a new filament);
- all free Arp2/3 are considered to be activated (by Act or other activation protein). Activated Arp2/3 bounds to filament side;
- all concentrations are uniform in the considered volume (constant at each point of the volume at the selected time moment t).

The schematic representation of this simplified model is given in Fig. 3.3. The model includes 9 types of molecular subsets (reagents), each with their own properties: ACG, ACF, FIB, FIP, ARP, ARF, CAP, CAF, COP.
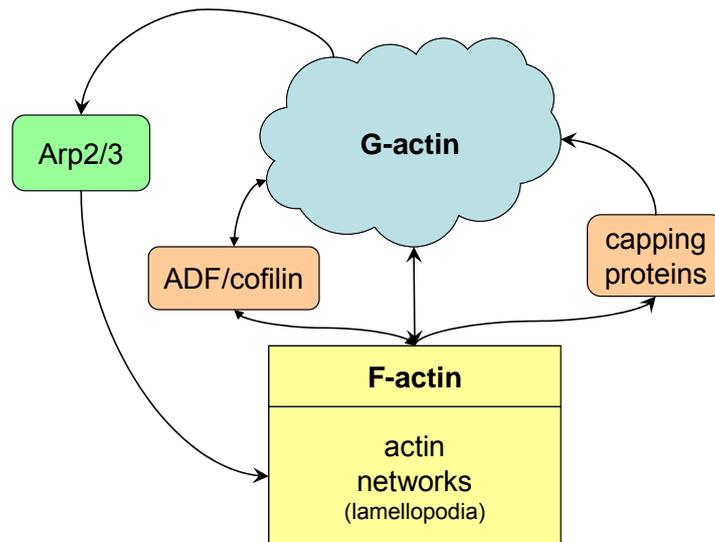


Figure 3.3. Schematic representation of a simplified biochemical network related to the actin polymerization process.

The reactions, which can be taken into account in the current model, are listed below.

1. Spontaneous nucleation, SNUC $\quad$ $3ACG \rightarrow 3ACF + FIB + FIP$

2. Association at barbed end, ASSB $\quad$ $FIB + ACG \rightarrow FIB + ACF$

3. Association at pointed end, ASSP $\quad$ $FIP + ACG \rightarrow FIP + ACF$

4. Dissociation at barbed end, DISB $\quad$ $FIB \rightarrow FIB + ACG$

5. Dissociation at pointed end, DISB $\quad$ $FIP \rightarrow FIP + ACG$

6. Branching, ARPB $\quad$ $ARP + ACF \rightarrow ARF + ACF + FIP$

7. Capping, CAPB $\quad$ $CAP + FIB \rightarrow CAF$

8. Severing on the filament, SEVR $\quad$ $ACF + COP \rightarrow ACG + COP + FIP + FIB$

9. Dissolve of short filaments[1], DEPO $\quad$ $a_1 \cdot ACF + a_2 \cdot ARF + a_3 \cdot CAF + FIB + FIP \rightarrow$
$$\rightarrow a_1 \cdot ACG + a_2 \cdot ARP + a_3 \cdot CAP$$

---

[1] This reaction is not evident. In simulation model it is realized in the following way. If after any action (dissociation, severing and branch detachment) the length of any filament becomes smaller than 2 actins, this filament dissolves.

**Differential equations.** The concentration of severing protein let's consider constant, and the time of the interaction of severing protein with a filament very small. With this assumptions the system can be described with 8 "players" (ACG, ACF, FIB, FIP, ARP, ARF, CAP, CAF) and 6 reactions (nucleation SNUC, association at barbed end ASSB, dissociation at pointed DISP, branching ARPB, capping CAPB, severing SEVR). As a non-evident 7th reaction the complete dissociation of short filaments with length of <3 actins can be considered (DEPO).

There are two ways for the analytical description of this system. In the first approach the number of dissolved filaments (denote as $X$) is estimated by the product of $k_{DEPO} \cdot FIP$. The value of the depolymerization rate $k_{DEPO}$ and average length of depolymerized filaments $a$ are found from simulation model.

$$\frac{\partial ACG}{\partial t} = -3 \cdot k_{SNUC} \cdot ACG^3 - k_{ASSB} \cdot ACG \cdot FIB - k_{ASSP} \cdot ACG \cdot FIP +$$
$$+ k_{DISB}\left(1 - \frac{ARF}{ARF + ACF}\right)FIB + k_{DISP} \cdot FIP + k_{SEVR} \cdot ACF \cdot COP + a \cdot X(\partial t) \tag{3.3a}$$

$$\frac{\partial ACF}{\partial t} = -\frac{\partial ACG}{\partial t} \tag{3.3b}$$

$$\frac{\partial FIB}{\partial t} = k_{SNUC} \cdot ACG^3 + k_{SEVR} \cdot ACF \cdot COP + k_{ARPB} \cdot ARP \cdot FIB - k_{CAPB} \cdot CAP \cdot FIB -$$
$$-\left(1 - \left(1 + a\frac{ARF}{ACF}\right)\frac{CAF}{FIP + ARF} + a\frac{ARF}{ACF}\right)X(\partial t) \tag{3.3c}$$

$$\frac{\partial FIP}{\partial t} = k_{SNUC} \cdot ACG^3 + k_{SEVR} \cdot ACF \cdot COP + k_{DISP}\left(\frac{ARF}{ARF + ACF}\right)FIP - X(\partial t) \tag{3.3d}$$

$$\frac{\partial ARP}{\partial t} = k_{DISP}\left(\frac{ARF}{ARF + ACF}\right)FIP - k_{ARPB} \cdot ARP \cdot FIB + a\frac{ARF}{ACF}X(\partial t) \tag{3.3e}$$

$$\frac{\partial ARF}{\partial t} = -\frac{\partial ARP}{\partial t} \tag{3.3f}$$

$$\frac{\partial CAP}{\partial t} = -k_{CAPB} \cdot CAP \cdot FIB + \left(1 + a\frac{ARF}{ACF}\right)\frac{CAF}{FIP + ARF}X(\partial t) \tag{3.3g}$$

$$\frac{\partial CAF}{\partial t} = -\frac{\partial CAP}{\partial t} \tag{3.3i}$$

However, this approach leaded to deviations between simulation and analytical modeling for long times. Therefore the second approach was developed and used. In this approach all different events, which can lead to depolymerization of short filaments are treated separately. The only empirical parameter, that is used in this approach, is the probability for the filament to have the smallest length (3 actins) $p_{=3}$, which should be defined from simulation.

To write down the system of differential equations it was assumed that:

- Short filaments (length < 3) can appear only as a result of severing or dissociation.

- Severing: we consider, that when ADF/cofilin severs the filament near filaments, new short filaments do not appear. F-actins of the short part directly go to G-actin pool. The constant concentration of COP is included into the rate constant $k_{SEVR}$

- Dissociation: the item for actins which go to G-actin pool during dissociation is:

$$k_{DIS} \cdot end \cdot (3 \cdot p_{=3} + p_{>3}) = k_{DIS} \cdot end \cdot (1 + 2 \cdot p_{=3}) \tag{3.4}$$

where $k_{DIS}$ − one of the dissociation speeds;

$end$ − concentration of the corresponding filament ends;

$p_{=3}$ − probability, that the length of a filament at current moment of time is 3;

$p_{>3}$ − probability, that the length of a filament at current moment of time is >3

The full system of differential equations for 8 "players" is

$$
\begin{cases}
\dfrac{\partial ACG}{\partial t} = -3 \cdot k_{SNUC} \cdot ACG^3 - k_{ASSB} \cdot ACG \cdot FIB + k_{DISP} \cdot FIP(1 + 2 \cdot p_{=3}) + k_{SEVR} \cdot ACF\left(1 + \dfrac{3}{l} + \dfrac{3}{l_b}\right) \\[3mm]
\dfrac{\partial ACF}{\partial t} = -\dfrac{\partial ACG}{\partial t} \\[3mm]
\dfrac{\partial FIB}{\partial t} = k_{SNUC} \cdot ACG^3 + k_{SEVR} \cdot ACF\left(1 - \dfrac{3}{l}\left(1 - \dfrac{ARF}{ACF}\right) - \dfrac{3}{l_b} \cdot \dfrac{FIB}{FIP + ARF}\left(1 - \dfrac{ARF}{ACF}\right)\right) + \\[3mm]
\qquad + k_{ARPB} \cdot ARP \cdot ACF - k_{CAPB} \cdot CAP \cdot FIB - k_{DISP} \cdot FIP \cdot \left(1 + 3 \cdot \dfrac{ARF}{ACF}\right) \cdot \dfrac{FIB}{FIP + ARF} \cdot p_{=3} \\[3mm]
\dfrac{\partial FIP}{\partial t} = k_{SNUC} \cdot ACG^3 + k_{SEVR} \cdot ACF\left(1 - \dfrac{1}{l}\left(3 - 6\dfrac{ARF}{ACF}\right) - \dfrac{1}{l_b}\left(3 - 6\dfrac{ARF}{ACF}\right)\right) - k_{DISP} \cdot FIP \cdot p_{=3} \\[3mm]
\dfrac{\partial ARP}{\partial t} = -k_{ARPB} \cdot ARP \cdot ACF + k_{SEVR} \cdot ACF\left(\dfrac{3}{l}\dfrac{ARF}{ACF} + \dfrac{3}{l_b}\dfrac{ARF}{ACF}\right) + k_{DISP} \cdot FIP \cdot 3\dfrac{ARF}{ACF} \cdot p_{=3} \\[3mm]
\dfrac{\partial ARF}{\partial t} = -\dfrac{\partial ARP}{\partial t} \\[3mm]
\dfrac{\partial CAP}{\partial t} = -k_{CAPB} \cdot CAP \cdot FIB + k_{SEVR} \cdot ACF \cdot 3\dfrac{CAF}{ACF}\left(1 - \dfrac{ARF}{ACF}\right) + \\[3mm]
\qquad + k_{DISP} \cdot FIP \cdot \left(1 + 3 \cdot \dfrac{ARF}{ACF}\right) \cdot \dfrac{CAF}{FIP + ARF} \cdot p_{=3} \\[3mm]
\dfrac{\partial CAF}{\partial t} = -\dfrac{\partial CAP}{\partial t}
\end{cases}
\tag{3.5}
$$

Using the known relation between FIB, FIP, ARF, CAF

$$FIB = FIP + ARF - CAF, \tag{3.6}$$

initial concentrations of actins, Arp2/3 and capping proteins (A, R and C respectively)

$$ACF = A - ACG \tag{3.7a}$$

$$ARP = R - ARF \tag{3.7b}$$

$$CAP = C - CAF \tag{3.7c}$$

and denoting $l$ – average length of the filament, $l_b$ – average length of a branch,

$$l = (A - ACG) / FIP \qquad (3.8a)$$

$$l_b = (A - ACG) / (FIP + AFR) \qquad (3.8b)$$

the system (3.5) can be simplified into the system of four linearly independent equations.

$$
\begin{cases}
\dfrac{\partial ACG}{\partial t} = -3 \cdot k_{SNUC} \cdot ACG^3 - k_{ASSB} \cdot ACG \cdot (FIP + ARF - CAF) + k_{DISP} \cdot FIP(1 + 2 \cdot p_{=3}) + \\[2mm]
\qquad + k_{SEVR} \cdot (A - ACG)\left(1 + \dfrac{3}{l} + \dfrac{3}{l_b}\right) \\[4mm]
\dfrac{\partial FIP}{\partial t} = k_{SNUC} \cdot ACG^3 + k_{SEVR} \cdot (A - ACG)\left(1 - \dfrac{1}{l}\left(3 - 6\dfrac{ARF}{A - ACG}\right) - \dfrac{1}{l_b}\left(3 - 6\dfrac{ARF}{A - ACG}\right)\right) - \\[2mm]
\qquad - k_{DISP} \cdot FIP \cdot p_{=3} \\[4mm]
\dfrac{\partial ARF}{\partial t} = k_{ARPB} \cdot (R - ARF) \cdot (A - ACG) - k_{SEVR} \cdot (A - ACG)\left(\dfrac{3}{l}\dfrac{ARF}{A - ACG} + \dfrac{3}{l_b}\dfrac{ARF}{A - ACG}\right) - \\[2mm]
\qquad - k_{DISP} \cdot FIP \cdot 3\dfrac{ARF}{A - ACG} \cdot p_{=3} \\[4mm]
\dfrac{\partial CAF}{\partial t} = k_{CAPB} \cdot (C - CAF) \cdot (FIP + ARF - CAF) - k_{SEVR} \cdot (A - ACG) \cdot 3\dfrac{CAF}{A - ACG}\left(1 - \dfrac{ARF}{A - ACG}\right) - \\[2mm]
\qquad - k_{DISP} \cdot FIP \cdot \left(1 + 3 \cdot \dfrac{ARF}{A - ACG}\right) \cdot \dfrac{CAF}{FIP + ARF} \cdot p_{=3}
\end{cases}
$$

$$(3.9)$$

### 3.3. Simulation models for biochemical reactions

#### 3.3.1. Monte Carlo simulation of the chemical reactions

To simulate the interactions between reagents the Gillespie's Monte Carlo approach was implemented (Gillespie, 1976). Several realizations were tried, including classical "first reaction", Gibson-Bruck's (Gibson and Bruck, 2000) and τ-leap (Gillespie, 2001) algorithms. Because of the relatively small number of reactions, and necessity to evaluate results of each reaction, Gibson-Bruck's approach, being the fastest exact simulation algorithm, has not provided any significant speeding up in comparison with the classical "first reaction". The τ-leap approach proved itself inapplicable in our case, because of small concentrations of some reagents (such as filaments binding sites: FIB and FIP).

All of them are based on calculation of concentration-dependent rates $a_i$, is the concentration-dependent reaction rate, which is proportional to the product of the reaction rate $k_i$ and the quantities of the reacting compounds. The product $a_i dt$ gives the probability for $i$-th reaction to occur in the infinitesimal time $dt$. These rates can be obtained from experimental rate constants $k$ using equations, which varies for different types of reactions (Gillespie, 1977). As was calculated for the considered model, these equations are (see reaction numbers in the section 3.2.2):

Reaction 1 (3 reagents): $\qquad a_i = k_i \cdot n_I \cdot (n_I - 1) \cdot (n_I - 2) \cdot V^{-2} \cdot N_A^{-2} \cdot 10^{12}$

Reactions 2, 3, 6, 7 (2 reagents): $\quad a_i = k_i \cdot n_I \cdot n_{II} \cdot V^{-1} \cdot N_A^{-1} \cdot 10^{6}$

Reactions 4, 5 (1 reagent): $\qquad a_i = k_i \cdot n_I$

In this equations $n_{I,II}$ – number of molecules of types $I$ and $II$, $V$ – considered volume in liters, $N_A$ – Avogadro number, $k_i$ has the dimensionalities: $M^{-2}s^{-1}$ (reaction 1), $M^{-1}s^{-1}$ (reactions 2, 3, 6, 7), and $s^{-1}$ (reactions 4, 5).

**"First reaction" algorithm.** In Gillespie's "first reaction" algorithm the putative times $\tau_i$ for each $i$-th reaction are generated using the assumption that the flow of reaction-events is Poisson one, and therefore the times between events are exponentially distributed. Using the method of inverse functions, the putative time $\tau_i$ for $i$-th reaction can be calculated as

$$\tau_i = - a_i^{-1} \, ln(\xi) , \qquad\qquad (1)$$

where $a_i$ is the concentration-dependent reaction rate, which is the product of the reaction rate $k_i$ and quantities of the reacting compounds; $\xi$ is the uniformly distributed random value within the range (0,1). The reaction with the smallest $\tau_i$ occurs and the system's time is increased by $\tau_i$.

Each reaction modifies simultaneously the parameters of the system (ACG, ACF, ARP etc.) and number of molecules in the filament, which participates the reaction.

**Modified "first reaction" algorithm.** It was decided to modify the Gillespie first reaction approach and include into it the events of systems mechanics recalculation as an additional "reaction". The modified approach combines the advantages of first reaction method with discrete-time mechanics recalculation. The idea of the method is introducing 2 parallel times: for reactions ($t_{react}$) and for mechanics ($t_{mech}$). The second one had small constant increment $\Delta t$, which is supposed to be much smaller then average discrete on reaction time: $\Delta t << mean(t_{react}^{i+1} - t_{react}^{i})$. After each reaction a number of mechanical movements are performed with discreet time $t_{mech}$ until $t_{mech} > t_{react}$. Then algorithm simulates the next reaction.

### 3.3.2. Simulation model regardless filament structures

The first simulation model developed was based on the formalism described in 3.2.2.

The following approximations have been made during simulation:

1. Each filament was represented only by the number of molecules it contains, it means: ACF, ARF and CAF. The structure-dependent events (for instance, the severing position and redistribution of the molecules in the daughter filaments) was simulated using probabilistic approach.

2. All considered free Arp2/3 complexes are assumed to be activated. Hence, they all can participate in branching.

3. The concentration of severing protein is considered to be constant, and the time of the interaction of severing protein with a filament very small.

4. Moreover, in this model we assume high concentration of profilin, which replaces ADP in the free G-actins, by ATP and so, "recharges" them for further polymerization cycle. Therefore we do not consider the ATP-recharging as an additional reaction, assuming relatively high rate of recharging.

With this assumptions the system can be described with 6 reactions (FORM, ASSB, DISP, ARPB, CAPB, SEVR) of 8 reagents (ACG, ACF, FIB, FIP, ARP, ARF, CAP, CAF). As a non-evident 7th reaction, the complete dissociation of short filaments with length less than 3 actins has been considered.

For the simplicity of the model it was assumed that the formation of new filaments occurs spontaneously by binding together of 3 G-actins (ACG) with a very low reaction rate. As a product of this reaction the active pointed and barbed ends (FIB and FIP) are created as well. For the simplicity, we considered average rates for the reactions of association and dissociation; therefore we use the averaged barbed end association (ASSB), which describes adding of actin to the barbed end, and averaged pointed end dissociation (DISP), removing of the actin from the filament. The binding of Arp2/3 (ARP) complex to the filament provides an additional barbed end (FIB) and replaces one Arp2/3 complex from ARP-pool to ARF-pool. Capping decreases the number of active barbed ends (FIB) in the system. Severing by ADC/cofilin performs the double function: on one hand it facilitates the dissociation by cutting out an actin and on another – it leads to increase of the number of uncapped filament barbed ends, therefore stimulating the polymerization. Severing and depolymerization can lead to the complete dissociation of a filament, if its length becomes less 3 ACF. To track this situation, after each of these reactions the lengths of the resulting filaments is checked and small filament dissociates. If dissociating filament contains Arp2/3 or capping proteins, they are freed.

### 3.3.3. Simulation model with structural filament representation

According to the plan of the developing simulation model of actin polymerization processes, the simulation algorithm, where structures of filaments are considered, has been developed. There are several purposes for doing this step:

- Reduce uncertainty of possible chemical reactions and their rates;
- The new variant of the algorithm should be suitable for processing of experimental data: to predict system's behavior or to determine unknown parameters.

The main idea for the new algorithm is to save the information about all actins, which are included into filaments, and about their mutual position. The list of the reagents with the corresponding abbreviations is given in Table 3.1.

Table 3.1. List of the reagents

| N | Abbreviation | Description |
|---|---|---|
| 1 | ATG | G actines in ATP FORM |
| 2 | ADG | G actines in ADP FORM |
| 3 | ATF | F actines in ATP FORM |
| 4 | ADF | F actines in ADP FORM |
| 5 | FTB | filament free barbed ends(with the last actin containing ATP) |
| 6 | FDB | filament free barbed ends(with the last actin containing ADP) |
| 7 | FTP | filament free pointed ends(with the last actin containing ATP) |
| 8 | FDP | filament free pointed ends(with the last actin containing ADP) |
| 9 | CAP | Free capping proteins (barbed end cappers) |
| 10 | CAF | Bound capping proteins |
| 11 | TEP | Testin (the pointed-end capper) in a free form |
| 12 | TEF | Testin (the pointed-end capper) in a filament-bound form |
| 13 | FOP | Formin (nucleator) |
| 14 | FOF | Formin in filament-bound form |
| 15 | ADC | Severing protein ADF/coffilin |

There are three possible variants for the filament barbed ends:

- Free barbed ends. This group can be divided into two sub-groups: FTB and FDB, which differ from each other by forms of last actins (let us to count actins in filaments from the pointed ends). The difference between these subgroups is significant in the dissociation reactions (see below).

- Capped barbed ends. Their concentration is always equal to the concentration of the bound capping proteins (CAF).

- Barbed ends with formins. To find their concentration the concentration of FOF is used.

Two alternatives are presumed for the pointed ends:

- Free pointed ends. Divided into two subgroups (FTP, FDP) in the same way as for barbed ends.

- Capped pointed ends. The concentration is equal to the concentration of testin in a bound form.

Now it is necessary to consider possible reactions for this system. In the table below reactions are given with their abbreviations and typical rate values.

Table 3.2. Considered reactions

| Number | Abbreviation | Description | Rate |
|--------|-------------|-------------|------|
| 1 | SNUC | Filament formation | $10^{-6}$ $\mu M^{-2}s^{-1}$ |
| 2 | ASTB | Association of ATP actin with barbed end | 11,6 $\mu M^{-1}s^{-1}$ |
| 3 | ASDB | Association of ADP actin with barbed end | 3,8 $\mu M^{-1}s^{-1}$ |
| 4 | ASTP | Association of ATP actin with pointed end | 1,6 $\mu M^{-1}s^{-1}$ |
| 5 | ASDP | Association of ADP actin with pointed end | 0,16 $\mu M^{-1}s^{-1}$ |
| 6 | ASTF | Association of ATP actin with bared end with formin | |
| 7 | DSTB | Dissociation of ATP actin at barbed end | 1,4 $s^{-1}$ |
| 8 | DSDB | Dissociation of ADP actin at barbed end | 7,2 $s^{-1}$ |
| 9 | DSTP | Dissociation of ATP actin at pointed end | 0,8 $s^{-1}$ |
| 10 | DSDP | Dissociation of ADP actin at pointed end | 0,27 $s^{-1}$ |
| 11 | CAPB | Capping of barbed end | 3,0 $\mu M^{-1}s^{-1}$ |
| 12 | TESP | Capping of pointed end by testin | |
| 13 | SEVR | Severing of filament by ADF/cofilin | |
| 14 | FMNB | Association of formin with barbed end | |
| 15 | TTOD | Change from ATF TO ADF in filaments | |
| 16 | DTOT | Change from ADF TO ATF | |

All reactions can be divides into several classes (assumptions for all reactions are also given):

**Filament spontaneous nucleation (SNUC):**

$$3 \cdot ATG \rightarrow 3 \cdot ATF + FTB + FTP .$$

It is assumed, that only actins with ATP can participate in filament formation. Result is filament with 3 ATP actins, which has free barbed and pointed ends.

**Association reactions:**

ASTB: $FTB(FDB) + ATG \rightarrow FTB^{+ATF}$

ASDB: $FTB(FDB) + ADG \rightarrow FDB^{+ADF}$

ASTP: $FTP(FDP) + ATG \rightarrow FTP^{+ATF}$

ASDP: $FTP(FDP) + ADG \rightarrow FDP^{+ADF}$

ASTF: $FOF + ATG \rightarrow FOF^{+ATF}$
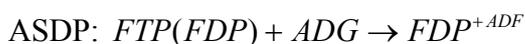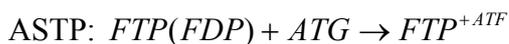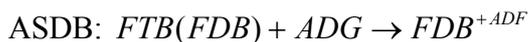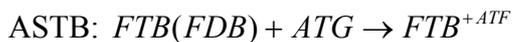
The reaction probability doesn't depend on the filament-ending actin, but depends on the form of the associated actin. Rates for these 4 reactions are considered as independent. The typical

values were found in the articles. Barbed ends with formin can react only with ATP actins, but reaction rate is higher, than in case of free barbed ends.

**Dissociation reactions:**

DSTB: $FTB^{+ATF} \rightarrow FTB(FDB) + ATG$

DSDB: $FDB^{+ADF} \rightarrow FTB(FDB) + ADG$

DSTP: $FTP^{+ATF} \rightarrow FTP(FDP) + ATG$

DSDP: $FDP^{+ADF} \rightarrow FTB(FDB) + ADG$
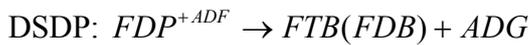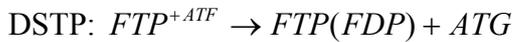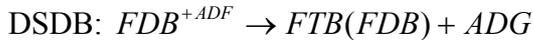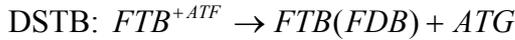
These reactions are reverse reactions for the corresponding associations. Their probabilities depend only on the type of ending actin at the free filaments end and independent on the next actins. If a filament becomes shorter than 3 actins, it dissociates and form free actins immediately.

**"Capping" reactions:**

CAPB: $FTB(FDB) + CAP \rightarrow CAF$

TESP: $FTP(FDP) + TEP \rightarrow TEF$

FMNB: $FTB(FDB) + FOP \rightarrow FOF$

There are no differences between various subgroups of free ends. The abbreviations CAF/TEF/FOF are used both for the corresponding proteins in the bound form and for the corresponding capped ends.

**Severing reaction:**

$ADC + ADF \rightarrow ADC + ADG + FTB(FDB) + FTP(FDP)$

Complexes of actins with ADC/cofilin are not considered. These proteins in the model are used for the regulation of the severing intensity. Short filaments, obtained after reaction, $(l < 3)$ dissociate immediately.

**Change of actins types:**

TTOD: $ATF \rightarrow ADF$

DTOT: $ADG \rightarrow ATG$

The change of F-actin forms (ATP or ADP associated) doesn't depend on neighboring actins. It's simulated as other chemical reactions with the corresponding reaction constant. If the last (first) actin of the filament is changed, the type of the corresponding filament end should be modified. Reaction constant for free actins is given per unit, i.e. concentration of profilin is included.

### *3.4. Mesoscale mechanical models of actin based bead propulsion*

#### 3.4.1. Hierarchy of the models

To be able to simulate bead (bacteria) propulsion it was decided to imitate the small volume of 3D-space filled with solution of proteins, filaments and a bead. This mesoscale model is base on two main blocks (see Fig. 3.4): the chemical model for molecular reactions and the mechanical model, representing mechanical motions and interactions. In this model filaments and the bead are considered as physical objects, described by their coordinates, orientations, velocities, friction tensors, etc. Free proteins are considered in terms of concentrations. For the moment it was decided to assume constant protein concentrations in the considered volume. In future the volume can be divided into smaller sub-volumes and the gradients of concentrations could be taken into account.
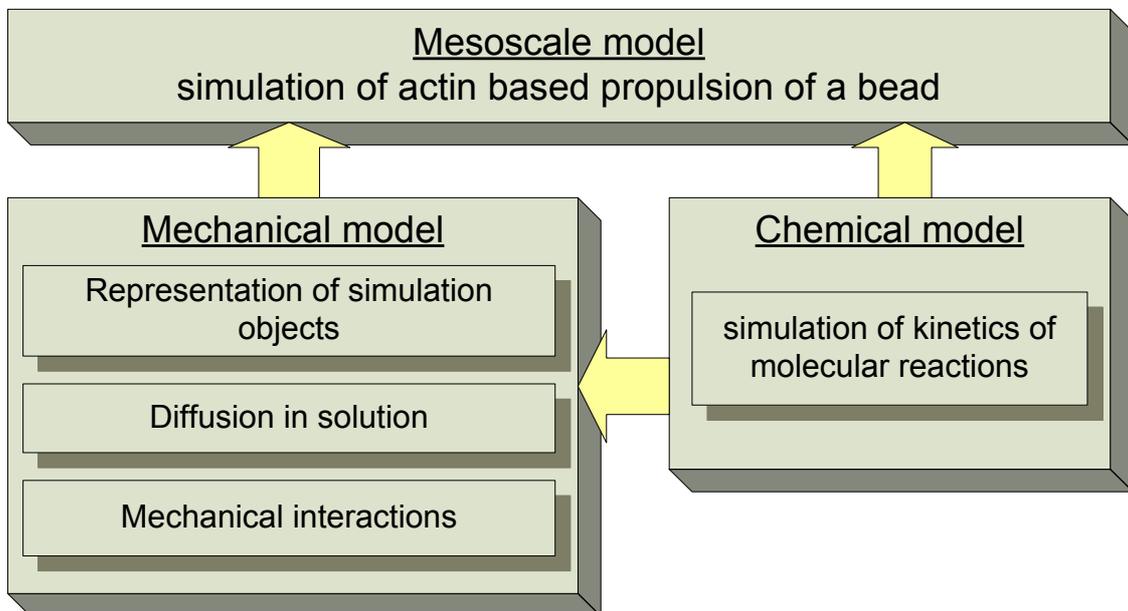


Figure 3.4. Hierarchy of the mesoscale model.

The model for reactions has been described in details in section 3.3.1 (modified Gillespie's "first reaction" method).

#### 3.4.2. Filaments and bead representation

**Filaments.** The actin filament can be approximated by a linear chain of G-actin monomers. G-actin is a plate like molecule with size is about 5.5×5.5×3.5 nm. Because of the twist of a filament, the filament diameter differs from 7nm to 9 nm. We consider the filament in our model as solid thin cylinder (see Fig. 3.5). As shown, filament cylinder consists of elementary cylinders that represent actin monomers.
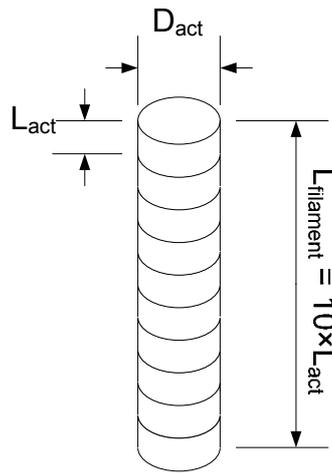
Figure 3.6. Representation of a filament consists of ten actin monomers.

The position of a filament in a space is described by the coordinates of the begin, filament length and orientation of the cylinder (see Fig. 3.6). The orientation of the cylinder can be defined by a rotation matrix that rotates global coordinate system $X_G Y_G Z_G$ to local coordinate system $X_L Y_L Z_L$ related with cylinder axis.
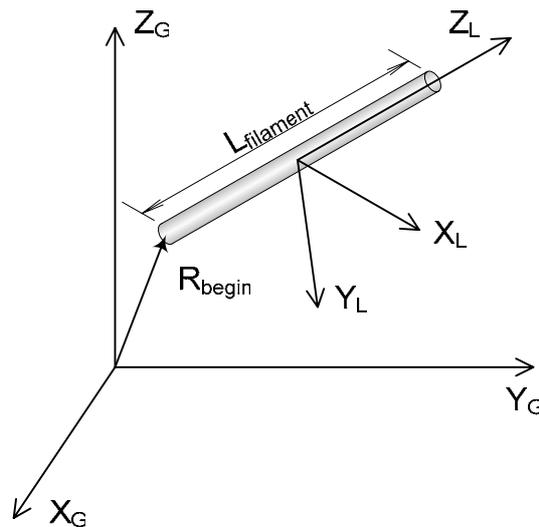


Figure 3.6. The filament is free oriented in space.

**Bead.** A polystyrene bead frafted with actin nucleators are used in experiment of actin based propulsion. We represent the bead by a sphere and positions of nucleators on the sphere surface by points (see Fig. 3.7.). Coordinates of nucleators and the sphere center are specified in the global coordinate system.
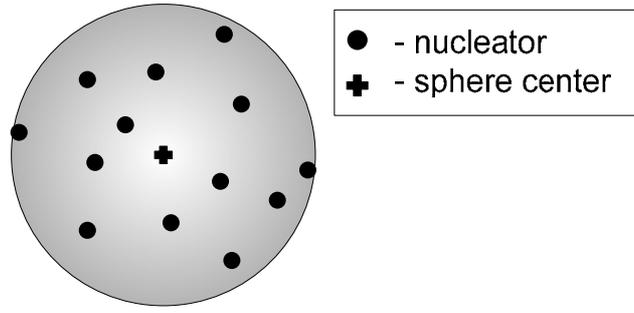
Figure 3.7. Bead representation as sphere.

### 3.4.3. Diffusion in solution

For simulation of diffusion in solution we uses the Langevin approach (Dünweg et al., 2003; Ermak and McCammon, 1978). The Langevin equations for translational (3.10) and rotational (3.11) motion of a Brownian particle are

$$m\frac{d^2r}{dt^2} = -\gamma_T \frac{dr}{dt} + F(r) + r^0 \tag{3.10}$$

$$\omega = \frac{d\varphi}{dt}$$
$$\frac{d(I\omega)}{dt} + [\omega \times I\omega] = -\gamma_R \omega + K(\varphi) + \varphi^0 \tag{3.11}$$

where

$m$ – mass of the particle;

$I$ – inertia tensor of the particle;

$r$ – radius-vector of the mass center;

$\varphi$ – rotational angle respectively to the mass center;

$\omega$ – rotational velocity;

$\gamma_T$ and $\gamma_R$ – friction tensors for translational and rotational motions respectively;

$F(r)$ – resultant force applied to the particle;

$K(\varphi)$ – sum moment of the forces, determined respectively mass center;

$r^0$ – noise process with $<r^0(t)> = 0$, $<r^0(t)r^0(t+s)> = 2\gamma_T k_B T\delta(s)$;

$\varphi^0$ – noise process with $<\varphi^0(t)> = 0$, $<\varphi^0(t)\varphi^0(t+s)> = 2\gamma_R k_B T\delta(s)$.

In the limit of high friction equations (3.10, 3.11) reduces to

$$\frac{dr}{dt} = \frac{1}{\gamma_T}F(r) + \frac{1}{\gamma_T}r^0 \tag{3.12}$$

$$\omega = \frac{1}{\gamma_R}K(\varphi) + \frac{1}{\gamma_R}\varphi^0. \tag{3.13}$$

Equations (3.12, 3.13) can be integrated by a simple explicit scheme

$$\Delta r(\Delta t) = \frac{\Delta t}{\gamma_T} F(r(t)) + \sqrt{2D_T \Delta t} \cdot r^G \qquad (3.14)$$

$$\Delta \varphi(\Delta t) = \frac{\Delta t}{\gamma_R} K(\varphi(t)) + \sqrt{2D_R \Delta t} \cdot \varphi^G \qquad (3.15)$$

where

$D_T$ and $D_R$ – diffusion tensors for translational and rotational motions respectively;

$\Delta t$ – integration time step;

$r^G$ – Gaussian distributed noise with $\mu = 0$, $\sigma = 1$;

$\varphi^G$ – Gaussian distributed noise with $\mu = 0$, $\sigma = 1$.

To estimate friction and diffusion tensors for the bead, the Stocks-Einstein equation can be used, which describes the movements of a spherical body in a viscous incompressible liquid

$$\frac{1}{\gamma_T} = \left\{ \begin{array}{ccc} \dfrac{1}{6\pi\eta R_{bead}} & 0 & 0 \\[2ex] 0 & \dfrac{1}{6\pi\eta R_{bead}} & 0 \\[2ex] 0 & 0 & \dfrac{1}{6\pi\eta R_{bead}} \end{array} \right\} \qquad (3.16)$$

$$D_T = k_B T \cdot \frac{1}{\gamma_T}$$

$$\frac{1}{\gamma_R} = \left\{ \begin{array}{ccc} \dfrac{1}{8\pi\eta R_{bead}^{\,3}} & 0 & 0 \\[2ex] 0 & \dfrac{1}{8\pi\eta R_{bead}^{\,3}} & 0 \\[2ex] 0 & 0 & \dfrac{1}{8\pi\eta R_{bead}^{\,3}} \end{array} \right\} \qquad (3.17)$$

$$D_R = k_B T \cdot \frac{1}{\gamma_R}$$

where $R_{bead}$ is the radius of the bead, $\eta$ – dynamical viscosity of the solution, $k$ – Boltzman's constant, $T$ – temperature of the solution.

Observed by Broesma estimations of friction and diffusion tensors for cylinder (Li and Tang, 2004) are used to apply to filament

$$\frac{1}{\gamma_T} = \left\{ \begin{array}{ccc} \dfrac{\ln(L_F/d_F)+C_\perp}{4\pi\eta L_F} & 0 & 0 \\[3mm] 0 & \dfrac{\ln(L_F/d_F)+C_\perp}{4\pi\eta L_F} & 0 \\[3mm] 0 & 0 & \dfrac{\ln(L_F/d_F)+C_\parallel}{2\pi\eta L_F} \end{array} \right\} \tag{3.18}$$

$$D_T = k_B T \cdot \frac{1}{\gamma_T}$$

$$\frac{1}{\gamma_R} = \left\{ \begin{array}{ccc} 3\dfrac{\ln(L_F/d_F)+C_R}{\pi\eta L_R{}^3} & 0 & 0 \\[3mm] 0 & 3\dfrac{\ln(L_F/d_F)+C_R}{\pi\eta L_R{}^3} & 0 \\[3mm] 0 & 0 & 0 \end{array} \right\} \tag{3.19}$$

$$D_R = k_B T \cdot \frac{1}{\gamma_R}$$

where $R_F$ is the radius of the filament, $L_F$ – the length of the filament, $C_\perp = 0.886$, $C_\parallel = -0.114$ and $C_R = -0.447$ – the end-correction coefficients.

### 3.4.4. Mechanical interactions

Forces in the model can be applied to simulation objects: filaments and bead. Four types of forces were suggested to describe interactions of objects between themselves and the medium. These types are (see Fig.3.8):

1) Repulsion force due to crossing of the bead with a filament. The value is proportional to the crossing and the force is directed normally to the surface of the object.

2) Repulsion force due to crossing of the bead with a wall. The value is proportional to the crossing and the force is directed normally to the surface of the object.

3) Repulsion force due to crossing of the filament with a wall. The value is proportional to the crossing and the force is directed normally to the surface of the object.

4) Elastic retraction force with finite durability, which simulates molecular linkage. If the force is higher then durability value – the linkage breaks.
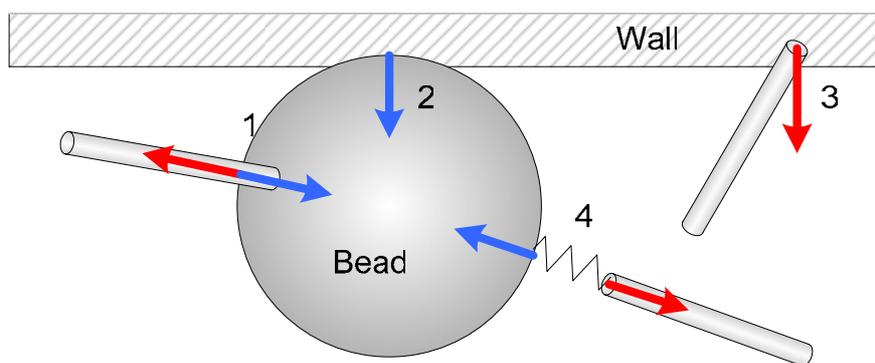
Figure 3.8. Types of forces which are considered for mechanical interactions:
1 − repulsion forces due to crossing of the bead with a filament; 2 − repulsion forces due to crossing of the bead with a wall; 3 − repulsion forces due to crossing of the filament with a wall; 4 − elastic retraction forces simulating molecular linkage.

The value of forces are calculated by following formula

$$F = K_j \delta \qquad (3.20)$$

where $\delta$ is distance of object intersection and $K_j$ − corresponding interaction coefficient ($j=1,2,3$). In the case of elastic retraction force $\delta$ is distance between linkage center and the considered object, $K_4$ − elastic coefficient of the molecular linkage.

### 3.4.5. Model for the reactions

To simulate the chemical reactions between reagents the Gillespie's Monte Carlo approach (Gillespie, 1976) was implemented. For this model we selected the most relevant proteins, usually used in laboratories for *in vitro* study of actin polymerization: actin, Arp2/3, ADC/cofilin, capping protein. More details of those were given above.

It was decided to modify the Gillespie first reaction approach and include into it the events of systems mechanics recalculation as an additional "reaction". The modified approach combines the advantages of first reaction method with discrete-time mechanics recalculation. The idea of the method is introducing 2 parallel times: for reactions ($t_{react}$) and for mechanics ($t_{mech}$). The second one had small constant increment $\Delta t$, which is supposed to be much smaller then average discrete on reaction time: $\Delta t << mean(t_{react}^{i+1} - t_{react}^{i})$. After each reaction a number of mechanical movements are performed with discreet time $t_{mech}$ until $t_{mech} > t_{react}$. Then algorithm simulates the next reaction.

# 4. SOFTWARE DEVELOPED

## *4.1. ActinPyreneFit – the experimental data analyzer*

The analytical model described in section 3.1 was implemented in a software tool ActinPyreneFit for the fast analysis of experimental pyrene-actin fluorescence. The screenshot of the program is given in Fig. 4.1. To assign the F-actin concentration with the fluorescence 2 additional fitted parameters has been introduced: background fluorescence B and time shift T. The relation between ACF and fluorescence then is:

$$f(t) = (F_0 - B)\frac{ACF(t-T)}{\max(ACF)} + B \qquad (4.1)$$

where $F_0$ – maximal experimental fluorescence, $\max(ACF)$ – maximal obtained $ACF$. For $t<T$ $ACF(t)$ was set to 0.
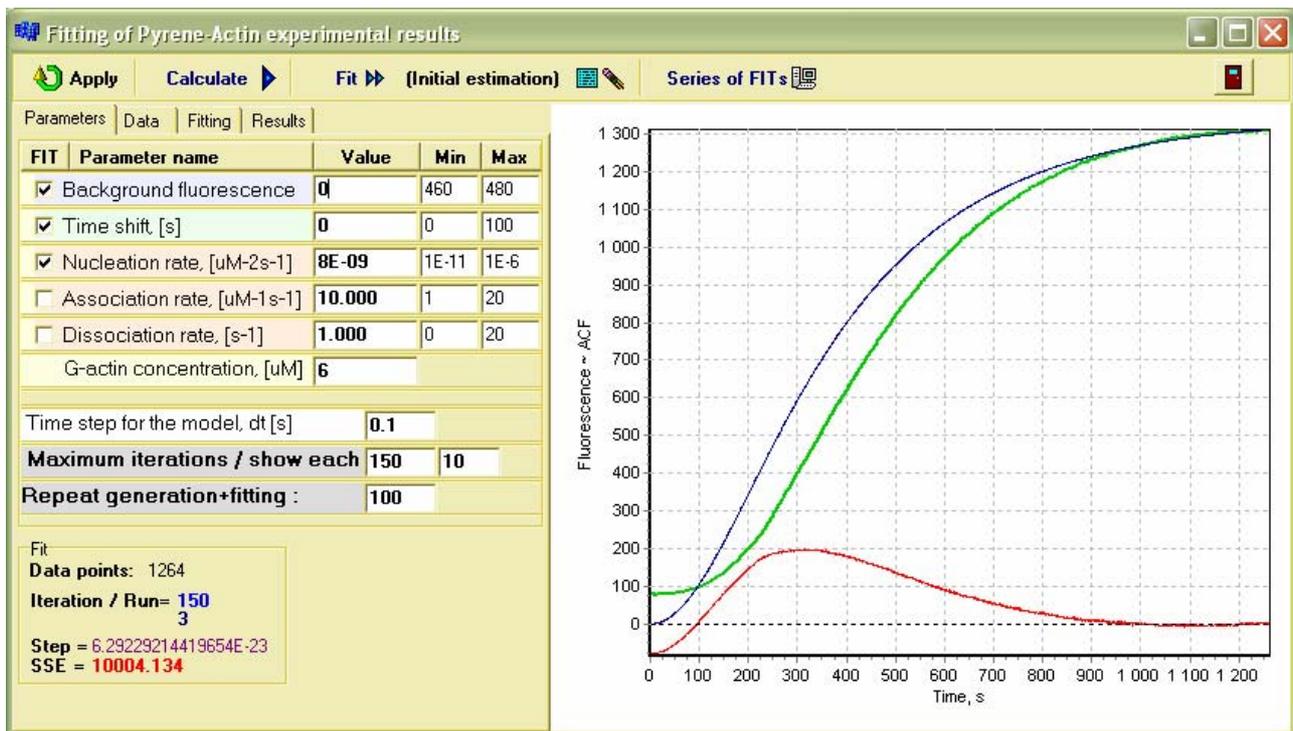


Figure 4.1. Screenshot of ActinPyreneFit.

On plots green line shows experimental data, blue line – model, red line – deviations (residuals).

The general scheme of work with the software is the following:

- The experimental data (time and fluorescence) should be pasted in the proper windows at the page "Data". Press [Apply].
- Select the fitted parameters, modify their boundaries and set constant parameters at page "Parameters". To apply changes press [Apply] or [Calculate].

- Set the number of fit iterations (100 – 200 is enough) and number of independent fits if necessary ("Repeat generation+fitting").
- To start single fit – press [Fit]. But we suggested to start a series of fits by pressing [Series of FITs].
- Collect the results at the page "Results". The first value in each row gives SSE for the fit, other gives $B$, $T$, $k_{SNUC}$, $k_{ASSB}$, $k_{DISB}$ respectively. The parameters with minimal SSE should be selected.

### *4.2. ActinSimChem – the simulator of the biochemical actin-related reactions*

In the simulation model for biochemical reactions each filament is characterized only by the numbers of F-actins (ACF), bound capping proteins (CAF) and bound Arp2/3 (ARF). The precise structure of the filament is unknown. However, the knowledge about the number of proteins in each filament is sufficient for Monte Carlo simulation of filament behavior during (de)polymerization. The model was realized as a part of software tool ActinSimChem. The screenshot of the developed program is given in Fig. 4.2.
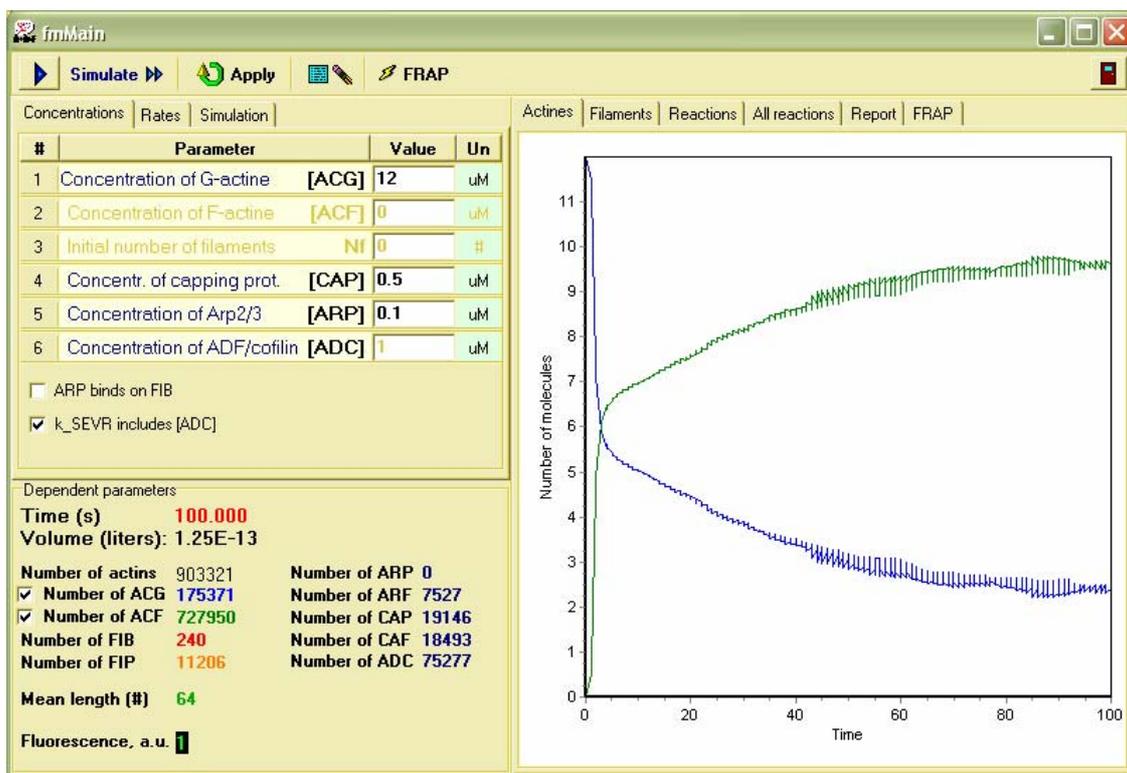


Figure 4.2. Screenshot of ActinSimChem with the results of several simulations of the actin polymerization. Blue line – G-actin, green – F-actin. Time is given in seconds.

### 4.3. ActinSimChem3DMech – the simulator of the mechanical interactions in actin assays

The resulted mesoscale model has been realized as a software tool ActinSimChem3DMech. The sources has been developed in Borland C++ Builder 6.0. To visualize the simulated 3D volume the free OpenGL package was used. See the screenshot of the software in Fig. 4.3.

The tasks, performed by this software, are:

1) Monte Carlo simulation of chemical reactions related to actin polymerization
2) Modeling of diffusion of filaments and their positions
3) Simulation of the filament-bead interactions using Newton dynamics.
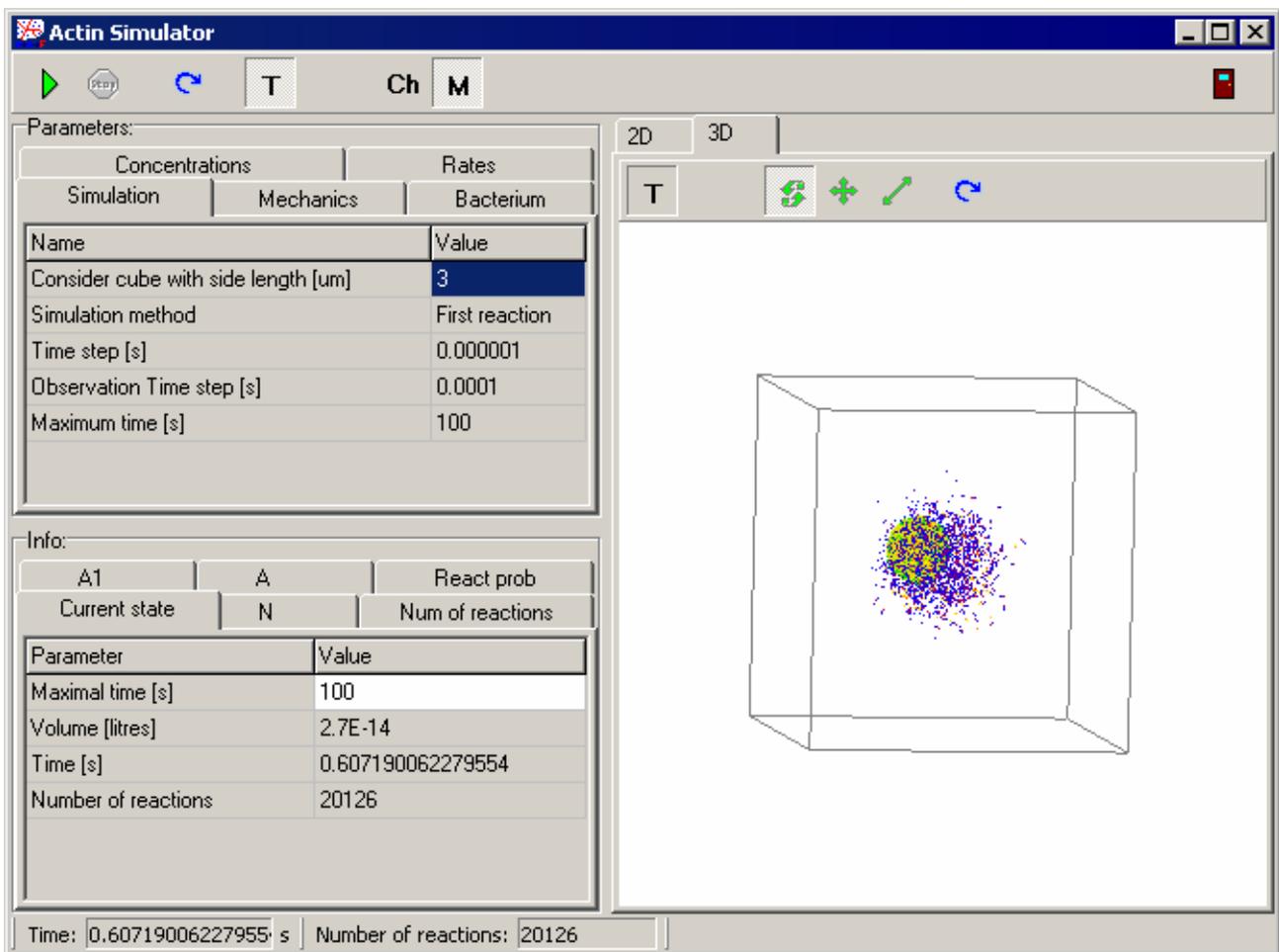


Figure 4.3. ActinSimChem3DMech software tool with the parameters of simulation in the left window and propulsion of bead in the right.

# 5. RESULTS

## 5.1. Verifications of the reaction models

### 5.1.1. Simple actin polymerization model: comparison of the analytical and simulation predictions

Consider first the analytical model described in section 3.2.1 and simulation model from section 3.3.2. It should be mentioned, that simulation model was used during the derivation of the analytical equations, especially empirical equation (3.2). However, after derivation of (3.2) the models operate completely independently, therefore we can use their comparison for the mutual verification.

Therefore below we compared the analytical model (Eqs. 3.1) with the simulation model from the section 3.3.2, with concentrations of ARP, CAP and COP set to 0 (no branching, no capping, no severing). The results are presented in Fig. 5.1 A, B.
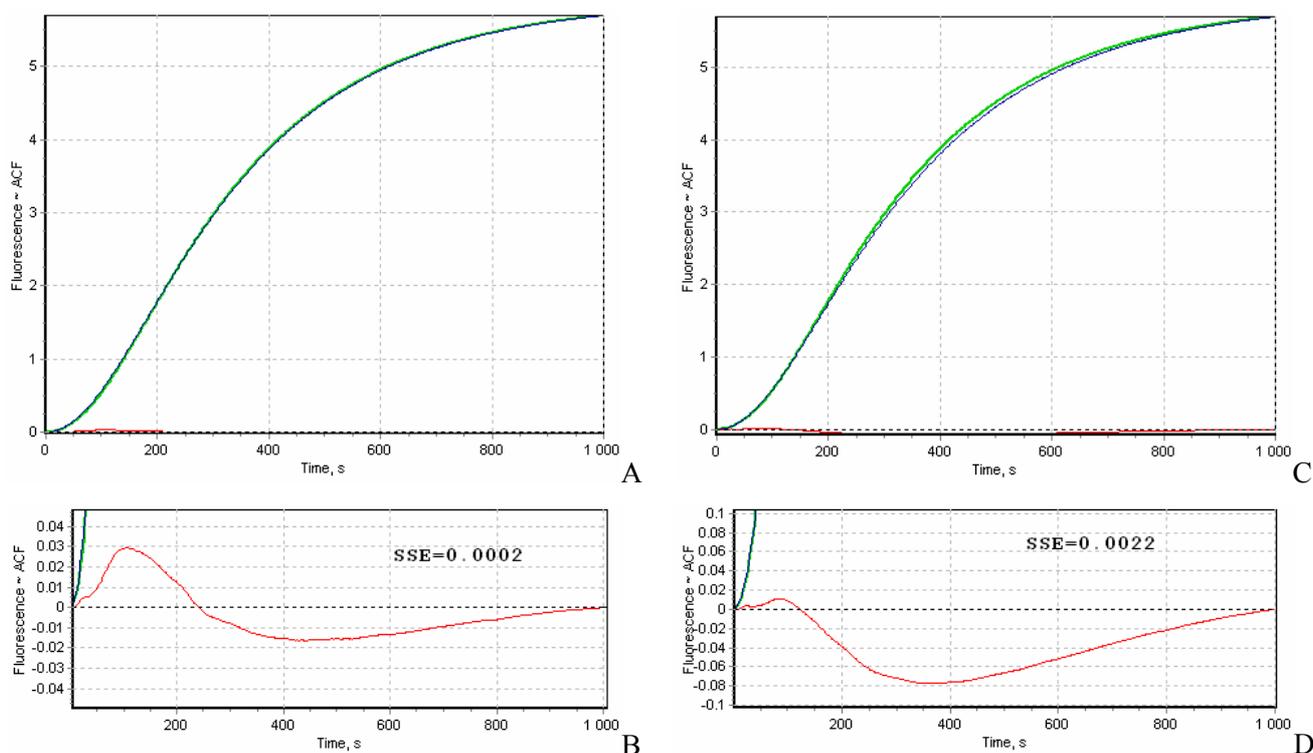


Figure 5.1. The comparison of the numerical simulation results (green line in (A) and (B)) and analytical modeling (dark blue lines in (A) and (B)). The experimental conditions: ACG0=6 μM, kSNUC=10-8 μM-2s-1, kASSB =10 μM-1s-1, kDISB =1 s-1, considered volume for the simulation model – cube with side of 15 μm. (A) shows the results for analytical model given by Eqs. 3.1, (B) shows the deviations between analytical and simulation models.  On plots (C) and (D) the same data are presented for the analytical model from (Carlsson et al., 2004).

The most intricate parameter of the analytical model is the probability $p_3$. To obtain the precise value of this parameter we have to know the filament length distribution at each time

moment or use empirical or simulation-based estimations. To describe the effect of this parameter (filament destruction) usually the following approximation is used in literature (Carlsson et al., 2004): in the nucleation reaction ACG concentration is replaced by $(ACG - k_{DISB}/k_{ASSB})$, where the subtrahend $k_{DISB}/k_{ASSB}$ is so called critical concentration. We tested this approach, and found that it leads to a certain inaccuracy of the model (see Fig. 5.1 C, D). The sum square error (SSE) for the Eqs. 3.1 is ~ 10 times smaller then for the approximated analytical model.

### 5.1.2. Simple actin polymerization model: comparison of the models with experimental data

The validity of the models (both simulation and analytical) was tested as well on the experimental data for actin polymerization. The experimental data was kindly provided by Sandrine Medves. The pyrene-actin data has been fitted by the model as described below ($k_{snuc}$ is modified), and the results of the best fit of the $k_{snuc} = 6.3 \times 10^{-09}$ is given in Fig. 5.2. The deviations (Fig. 5.2 B) are approximately at the order of magnitude of the stochastic noise.



A



B
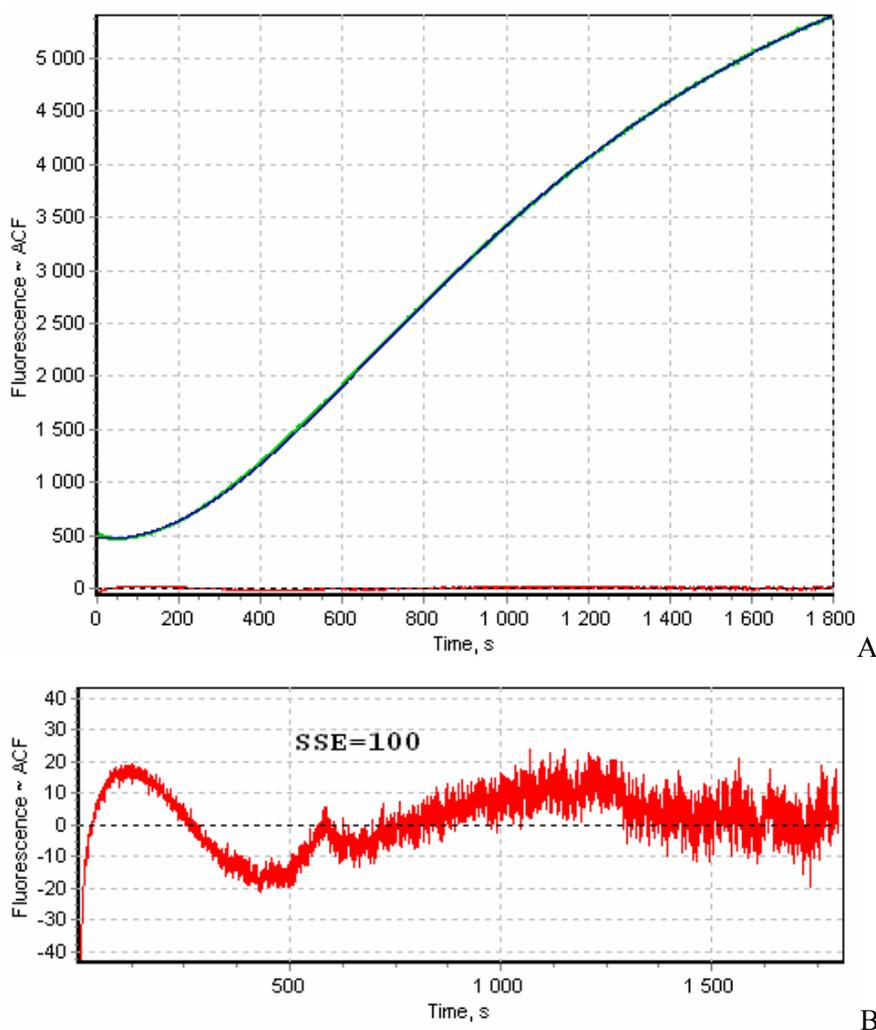
Figure 5.2. (A) The comparison of the analytical modeling (dark blue) and experimental data (green) for pure actin system (3 μM actin, data series 16 from Sandrine Medves). Plot (B) presents deviations between the model and experimental results.

### 5.1.3. Verification of the model describing branching, capping and severing

Once again the analytically obtained results (Eqs. 3.9) were compared with the results of simulation modeling (section 3.3.2). One of the examples of numerical experiment is presented below.
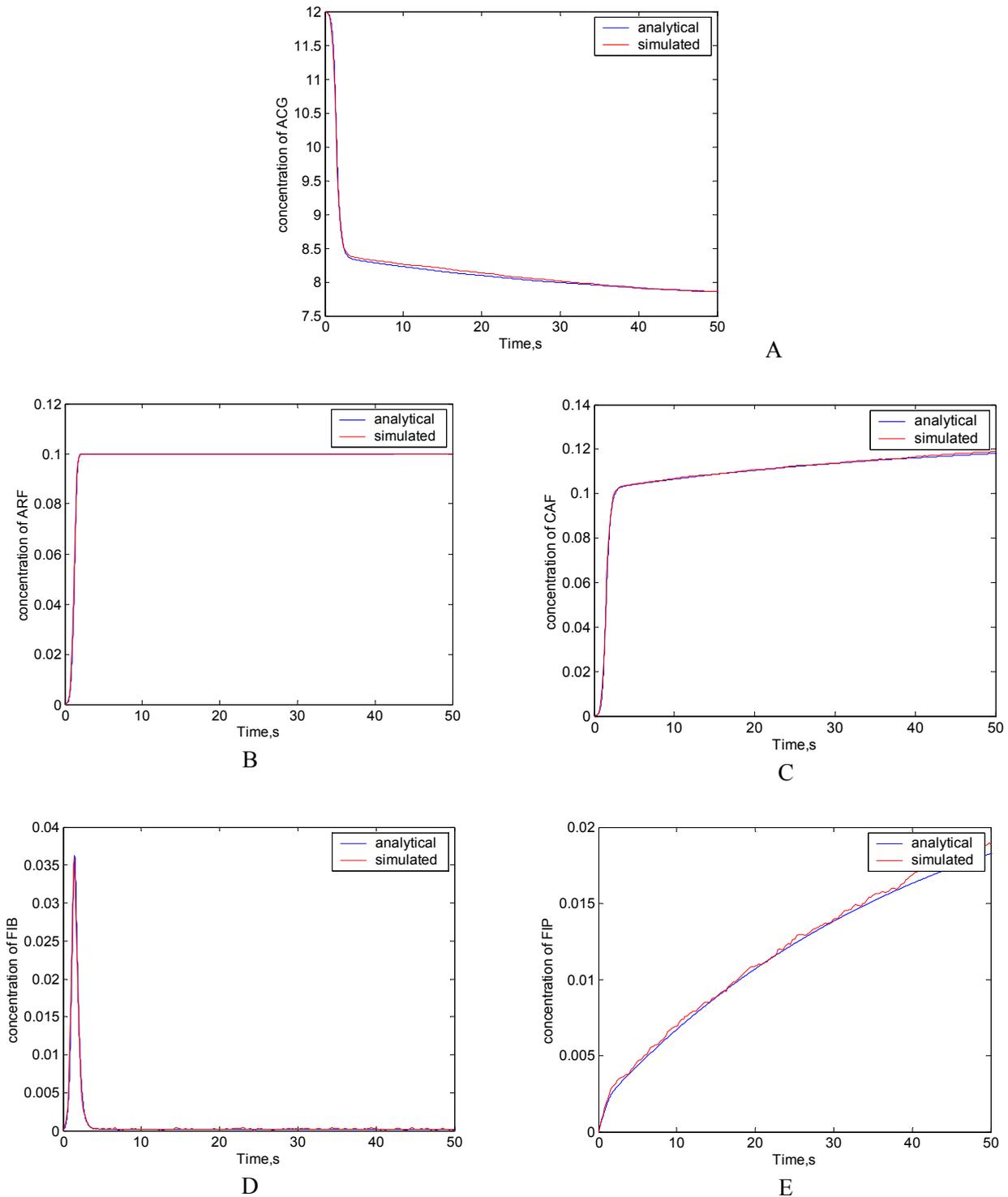


Figure 5.3. Comparison of the modeling results: blue line − analytical modeling, red line − simulation.

Initial concentrations: $A = 12$ μM, $R = 0.1$ μM, $C = 1$ μM.

Rate constants:

$$k_{SNUC} = 1 \cdot 10^{-6} \, \mu M^{-2} s^{-1}$$
$$k_{ASSB} = 10 \, \mu M^{-1} s^{-1}$$
$$k_{DISP} = 0.6 s^{-1}$$
$$k_{CABP} = 3 \, \mu M^{-1} s^{-1}$$
$$k_{SEVR} = 2.3 \cdot 10^{-6} \, s^{-1}$$

Note, that severing rate includes the concentration of COF.

It can be seen, that the behaviors of two models are perfectly in agreement.

Two stages can be seen for this particular numerical experiment from the concentration dynamics. The first is characterized by rapid filament growth just after first filament nucleation. The reason is in fast attachment of free Arp2/3 (we suppose that all free Arp2/3 are activated) to the new filament, producing more barbed ends and so − increasing the speed of filament formation. After the pool of free Arp2/3 is empty, the second stage of dynamics begins. Free barbed ends are almost completely capped by capping proteins (see their behavior in Fig. 3D) and the filament growth is almost completely dependent barbed ends which appear after severing. These factors lead to the smooth filament growth, starting approximately after 4 seconds after initial nucleation (Fig. 3A).

### 5.2. Experimental data analysis

#### 5.2.1. Correlation between parameters

To find possible correlation between fitted rate constants the fitting was performed on the data obtained by the simulation modeling with known rates. The following conclusions have been made after analysis of the results of 200 independent fitting runs.
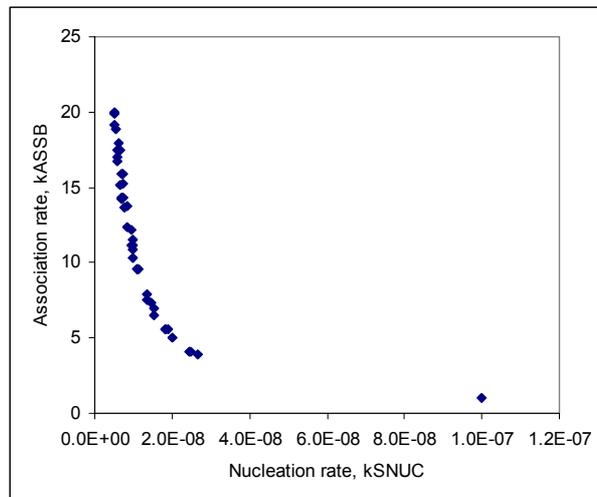


Figure 5.4. Scatter diagram of 2 parameters ($k_{ASSB}$ and $k_{SNUC}$) obtained in 80 independent fits.

1. Association rate ($k_{ASSB}$) is noticeably correlated with nucleation rate ($k_{SNUC}$). The correlation is depicted by scatter diagram of the found 80 best solutions in Fig. 5.4. The relation between the parameters can by approximated by the expression $k_{ASSB} \approx \alpha \cdot k_{SNUC}^{-1}$.

2. The dynamics of F-actin growth is not sensitive to the dissociation rate ($k_{DISB}$), therefore its determination via this type of experiments is questionable.

### 5.2.2. Some preliminary results of data analysis

**Sept's data.** The first series of the experimental data for the analysis was obtained from (Sept and McCammon, 2001) (see Fig. 5.5 A). The data was fitted by the model with $k_{ASSB} = 10 \; \mu M^{-1} s^{-1}$ and $k_{DISB} = 1 \; s^{-1}$.



A



B
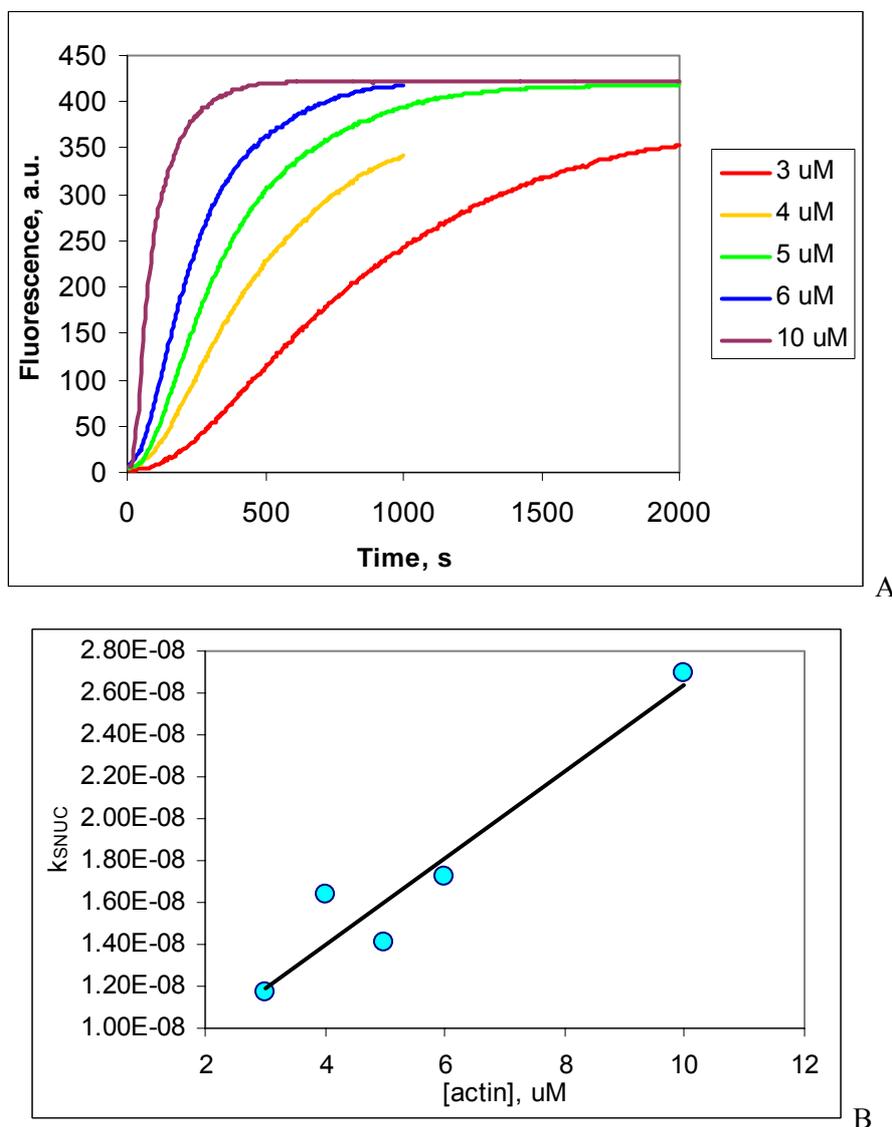
Figure 5.5. Experimental data for pure actin systems with different concentrations from (Sept and McCammon, 2001) (A).And found $k_{SNUC}$ after fitting of the data with constant $k_{ASSB}$ and $k_{DISB}$. uM stands for μM.

It can be seen that the nucleation rate linearly dependents on the concentration. This effect can be the evidence of the linear dependence between considered nucleation rate and actin concentration, and therefore suggests, that the minimal nucleus for the polymerization is 4-actin filament. The reaction of the nucleation is then: $4ACG \rightarrow 4ACF + FIB + FIP$. However, further experimental study should be performed to avoid possible experimental inaccuracies and artifacts.

**Sandrine's data.** The data were obtained by Sandrine during her experiments with forming, testin and CytoB proteins. To estimate the nucleation rate for the pure actin samples the following data sets have been used: 8, 10, 16, 18, 59. The resulted value and standard deviation are

$k_{SNUC} = (6.29 \pm 0.46) \times 10^{-9}\ \mu M^{-2} s^{-1}$

The found nucleation rate was compared with the results coming from data series 1 (formin), 3, 4 (testin-Nt), 7 (testin-Nt + CytoB), and 2 (formin + CytoB). The association and dissociation rates were hold constant $k_{ASSB} = 10\ \mu M^{-1} s^{-1}$ and $k_{DISB} = 1\ s^{-1}$. The results are summarized in Fig. 5.6.
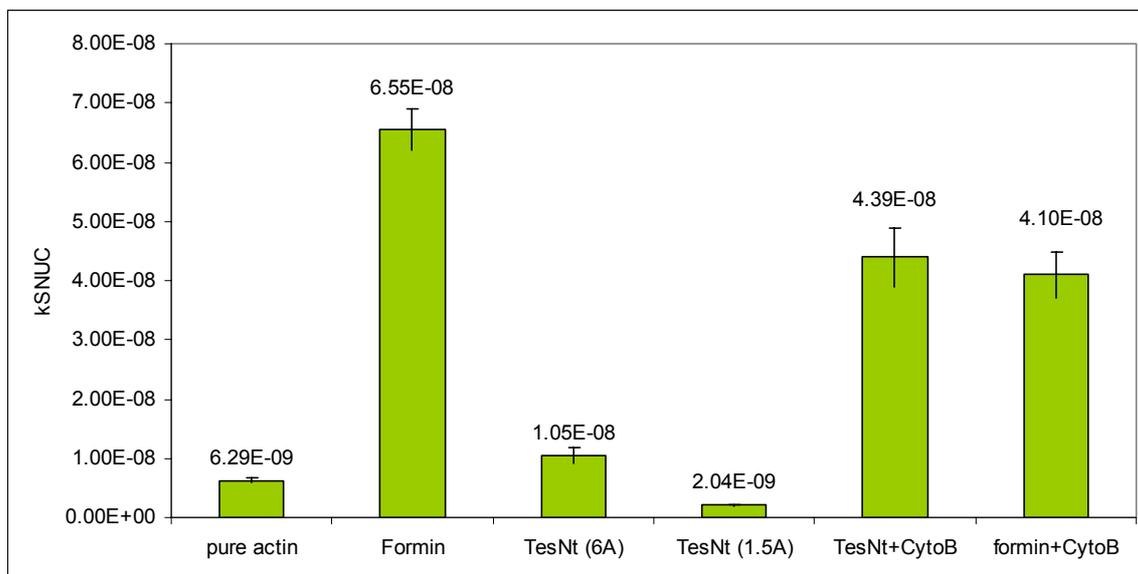


Figure 5.6. The determined $k_{SNUC}$ for different experimental systems.
For pure actin the 8, 10, 16, 18, 59 series were used, formin – series 1, testin-Nt (6μM of actin) – series 4, testin-Nt (1.5μM of actin) – series 3, testin-Nt + CytoB – series 7, and finally formin + CytoB – series 2.

From the presented results it can be conclude that testin-Nt does not change the nucleation rate. However formin and CytoB have both significant effects on the nucleation.

**Romero's data.** The data obtained by (Romero et al., 2004) on the system containing actin 1.5 μM, and formin (FH2) 40 nM, was fitted, assuming that formin change only the nucleation speed and does not influence the polymerization rate (the association and dissociation rates were hold constant $k_{ASSB} = 10\ \mu M^{-1} s^{-1}$ and $k_{DISB} = 1\ s^{-1}$). Interestingly the obtained fit was quite good, see Fig 7, with SSE=2.1. Determined $k_{SNUC} = 1.24 \times 10^{-7}\ \mu M^{-2} s^{-1}$. To distinguish between formin effect as

a nucleator and stimulator of association, the reference experiment with the same concentration of actins should be performed and analyzed simultaneously.
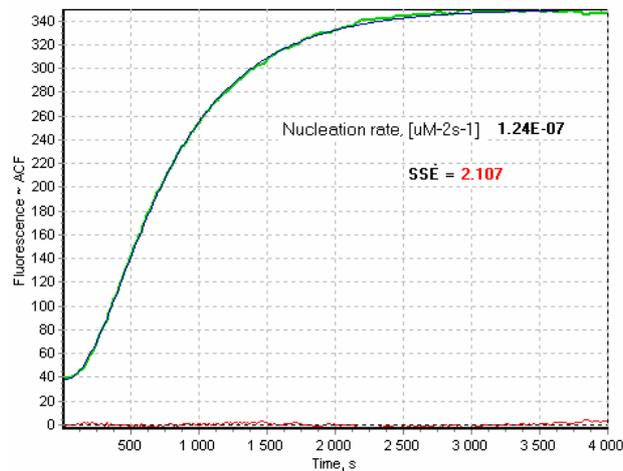


Figure 5.7. The obtained fit of the Romero's data (Romero et al., 2004) with $k_{SNUC} = 1.24 \times 10^{-7}$ $\mu M^{-2} s^{-1}$ and constant $k_{ASSB} = 10$ $\mu M^{-1} s^{-1}$ and $k_{DISB} = 1$ $s^{-1}$.

### 5.3. Results of a simulation of mechanical interactions

To be able to show generation of force applied to bead the following modified system was proposed. It was assumed that the solution viscosity is 1000 times higher and only half of the bead is frafted by actin nucleators. High solution viscosity prevents filament diffusion and leads to forming a actin gel layer around the bead. No uniform covering of the bead allows show up systematic motion of the bead. Fig 4.4 illustrates the time evolution of the polymerization and the resulted bead propulsion.
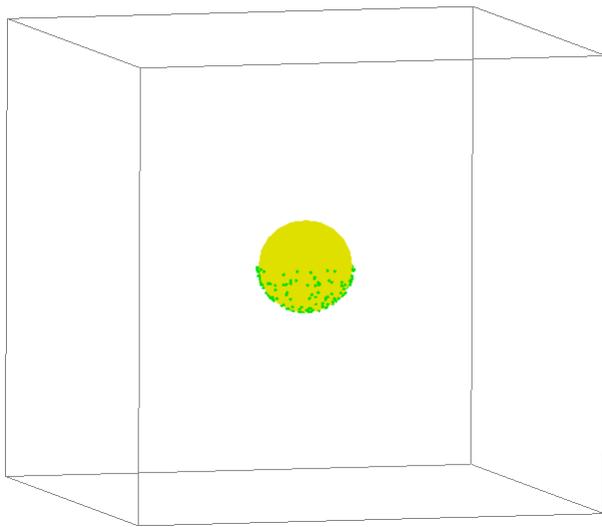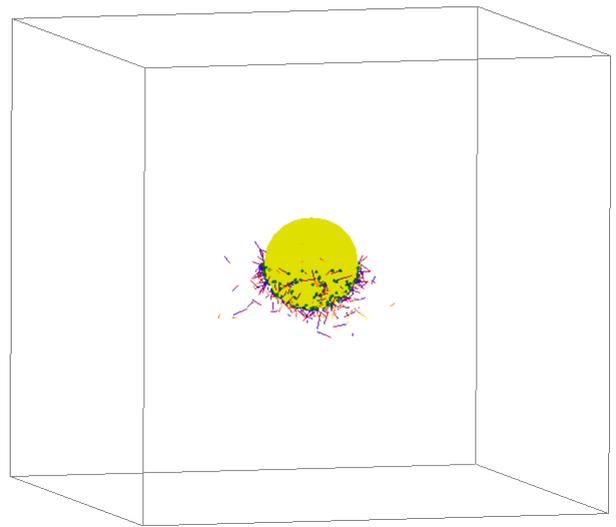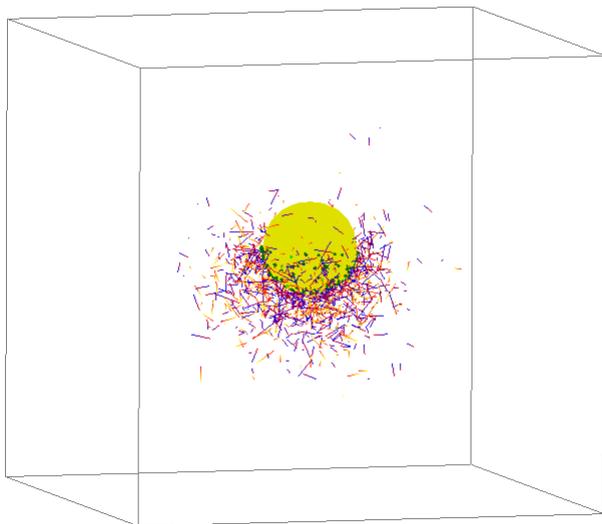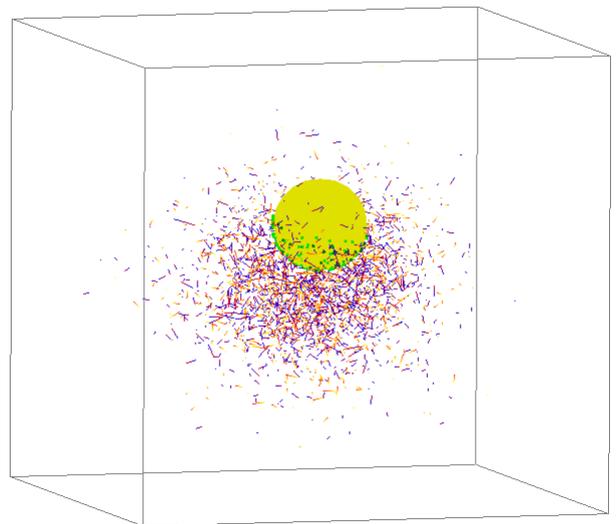
Figure 4.4. Time evolution of the bead-containing system:

A − at start time, B − approximately 1 s after simulation, C − 5 s, D − 10 s.

## 6. SUMMARY AND SUGGESTIONS FOR THE FURTHER RESEARCH

### *6.1. Summary*

From the very beginning this project was planned as a basis for a startup in collaboration of the Luxemburg scientific institutions (CRP-Sante, University) and Department of Systems Analysis, Belarusian State University (Belarus). The financial support by the FNR allows us to install the new fruitful scientific network between the above-mentioned institutions; it promotes the knowledge transfer, which was mutually beneficial.

The important point is that the study started under this project is still going and hopefully will lead to some advances in the study of actin polymerization.

Below we tried to summarize the results, achieved in the framework of the FNR project.

1. The simulation and analytical models which describes the actin polymerization has been developed and applied for experimental data analysis.

2. The *ab initio* model of mechanical interactions in actin polymerization assays has been developed, but needs further enhance – it's computational complexity strongly recommends to use a high speed computational cluster for the simulation.

3. The results of the work has been submitted (and presented) to two conferences:

   a. P. Nazarov, M. Yatskou, E. Barsukov, E. Ivashkevich, A. Golovaty, V. Apanasovich, E. Friederich. . Developing mathematical models, algorithms and programmig tools for analysis of actin based motility. Proceedings of 3rd International Workshop on: Mathematical Modeling of Actin- Based Modifity, 2006, Vienna, Austria, p.13 (*oral presentation*)

   b. A.A. Golovaty, P.V. Nazarov, M.M. Yatskou, V.V. Apanasovich, E. Friederich Simulation and analytical models for the analysis of in vitro actin polymerization. 8th International Conference Computer Data Analysis and Modeling: Complex Stochastic Data and Systems, 2007, Minsk, Belarus (*poster presentation*)

4. Currently two articles are in progress:

   a. P.V. Nazarov, A.A. Golovaty, M.M. Yatskou, V.V. Apanasovich, E. Friederich Model development and simulation-based analysis of *in vitro* actin polymerization.

   b. E. Barsukov, P.V. Nazarov, E. Ivashkevich, M. Yatskou, V. Apanasovich, E. Friederich, Mechanically justified simulation of actin-based bead propulsion.

## 6.2. Future plans

To study intrinsic and non-obvious properties of actin-filament systems, the aging of monomers should be taken into account. Therefore, the first step in enhancement of the molecular-scale model will be introduction of ATP and ADP containing actins. This will significantly increase the number of reactions. Moreover, it will make impossible the use of the biochemical model without structural model of actin filaments. The structural model should include precise positions of all ATP and ADP-containing actins, ATP and ADP containing barbed and pointed ends.

Moreover, in the future model it is planned to include testin (as a capper of pointed end), profilin (ATP-ADP exchanger), ActA (Arp2/3 activator) and other relevant molecular species.

The enhancement of the mesoscale mechanical model should go in two directions. First – by applying filament-filament interactions and concentrations gradients, and second – building up the parallel algorithm, able to work on the computational cluster.

Improved models should be used for analysis, or at least simulation of experimental FRAP data. The model for FRAP should be improved. The real structures of filaments and short filament diffusion should be taken into account.

# 7. REFERENCES

Alberts, J.B.; Odell, G.M. (**2004**) In silico reconstitution of Listeria propulsion exhibits nano-saltation. *PLoS Biol.*, 2(12), e412.

Atilgan, E.; Wirtz, D.; Sun, S.X. (**2006**) Mechanics and dynamics of actin-driven thin membrane protrusions. *Biophys. J.*, 90(1), 65-76.

Barkai, N.; Leibler, S. (**2000**) Circadian clocks limited by noise. *Nature*, 403(6767), 267-268.

Bartles, J.R.; Zheng, L.; Li, A.; Wierda, A.; Chen, B. (**1998**) Small espin: a third actin-bundling protein and potential forked protein ortholog in brush border microvilli. *J. Cell. Biol.*, 143(1), 107-119.

Bernheim-Groswasser, A.; Wiesner, S.; Golsteyn, R.M.; Carlier, M.F.; Sykes, C. (**2002**) The dynamics of actin-based motility depend on surface parameters. *Nature*, 417(6886), 308-311.

Berro, J.; Martiel, J.L. (**2005**) In silico model for actin filament assembly based on molecule population dynamics. *FEBS/ESF Workshop on Integrated Approaches in Cytoskeleton Research*, 32.

Brieher, W.M.; Coughlin, M.; Mitchison, T.J. (**2004**) Fascin-mediated propulsion of Listeria monocytogenes independent of frequent nucleation by the Arp2/3 complex. *J. Cell. Biol.*, 165(2), 233-242.

Cameron, L.A.; Robbins, J.R.; Footer, M.J.; Theriot, J.A. (**2004**) Biophysical parameters influence actin-based movement, trajectory, and initiation in a cell-free system. *Mol. Biol. Cell*, 15(5), 2312-2323.

Carlier, M.F.; Pantaloni, D.; Korn, E. (**1987**) The mechanism of ATP hydrolysis acompanying the polymerization of MG-actin and Ca-actin. *J. Biol. Chem.*, 262, 3052-3059.

Carlier, M.F.; Wiesner, S.; Le Clainche, C.; Pantaloni, D. (**2003**) Actin-based motility as a self-organized system: mechanism and reconstitution in vitro. *C. R. Biol.*, 326(2), 161-170.

Carlsson, A.E. (**2001**) Growth of branched actin networks against obstacles. *Biophys J*, 81(4), 1907-1923.

Carlsson, A.E.; Wear, M.A.; Cooper, J.A. (**2004**) End versus side branching by Arp2/3 complex. *Biophys J*, 86(2), 1074-1081.

Carlsson, A.E. (**2005**) The effect of branching on the critical concentration and average filament length of actin. *Biophys J*, 89(1), 130-140.

Carlsson, A.E. (**2006**) Stimulation of actin polymerization by filament severing. *Biophys. J.*, 90(2), 413-422.

Carrier, T.A.; Keasling, J.D. (**1999**) Investigating autocatalytic gene expression systems through mechanistic modeling. *J. Theor. Biol.*, 201(1), 25-36.

DesMarais, V.; Ghosh, M.; Eddy, R.; Condeelis, J. (**2005**) Cofilin takes the lead. *J. Cell Sci.*, 118(Pt 1), 19-26.

Dünweg, B.; (eds.), D.P.L.; (eds.), A.M. (**2003**) Langevin methods. *Computer simulations of surfaces*

*and interfaces, proceedings of the NATO Advanced Study Institute / Euroconference,*

*Albena, Bulgaria, September 2002, Kluwer Academic Publishers,*

*Dordrecht / Boston / London*, 77-92.

Edelstein-Keshet, L.; Ermentrout, G.B. (**1998**) Models for the length distributions of actin filaments: I. Simple polymerization and fragmentation. *Bull. Math. Biol.*, 60(3), 449-475.

Ermak, D.L.; McCammon, J.A. (**1978**) Brownian dynamics with hydrodynamic interactions. *J. Chem. Phys.*, 69, 1352-1360.

Ermentrout, G.B.; Edelstein-Keshet, L. (**1998**) Models for the length distributions of actin filaments: II. Polymerization and fragmentation by gelsolin acting together. *Bull. Math. Biol.*, 60(3), 477-503.

Gerbal, F.; Chaikin, P.; Rabin, Y.; Prost, J. (**2000**) An elastic analysis of Listeria monocytogenes propulsion. *Biophys. J.*, 79(5), 2259-2275.

Giardini, P.A.; Fletcher, D.A.; Theriot, J.A. (**2003**) Compression forces generated by actin comet tails on lipid vesicles. *Proc. Natl. Acad. Sci. USA*, 100(11), 6493-6498.

Gibson, M.A.; Bruck, J. (**2000**) Efficient exact stochastic simulation of chemical systems with many species and many channels. *J. Phys. Chem. A*, 104, 1876-1889.

Giganti, A.; Friederich, E. (**2003**) The actin cytoskeleton as a therapeutic target: state of the art and future directions. *Prog. Cell Cycle Res.*, 5, 511-525.

Giganti, A.; Plastino, J.; Janji, B.; Van Troys, M.; Lentz, D.; Ampe, C.; Sykes, C.; Friederich, E. (**2005**) Actin-filament cross-linking protein T-plastin increases Arp2/3-mediated actin-based movement. *J. Cell Sci.*, 118(Pt 6), 1255-1265.

Gillespie, D.T. (**1976**) A general method for numerically simulating the stochastic time evolution of coupled chemical reactions. *J. Comput. Phys.*, 22, 403-434.

Gillespie, D.T. (**1977**) Exact stochastic simulation of coupled chemical reactions. *J. Phys. Chem.*, 81(25), 2340-2361.

Gillespie, D.T. (**2001**) Approximate accelerated stochastic simulation of chemically reacting systems. *J. Chem. Phys.*, 115(4), 1716-1733.

Helfer, E.; Panine, P.; Carlier, M.F.; Davidson, P. (**2005**) The interplay between viscoelastic and thermodynamic properties determines the birefringence of F-actin gels. *Biophys. J.*, 89(1), 543-553.

Higgs, H.N.; Pollard, T.D. (**1999**) Regulation of actin polymerization by Arp2/3 complex and WASp/Scar proteins. *J. Biol. Chem.*, 274(46), 32531-32534.

Higgs, H.N.; Pollard, T.D. (**2001**) Regulation of actin filament network formation through ARP2/3 complex: activation by a diverse array of proteins. *Annu. Rev. Biochem.*, 70, 649-676.

Hucka, M.; Finney, A.; Bornstein, B.J.; Keating, S.M.; Shapiro, B.E.; Matthews, J.; Kovitz, B.L.; Schilstra, M.J.; Funahashi, A.; Doyle, J.C.; Kitano, H. (**2004**) Evolving a lingua franca and associated software infrastructure for computational systems biology: the Systems Biology Markup Language (SBML) project. *Syst Biol (Stevenage)*, 1(1), 41-53.

Janji, B.; Giganti, A.; De Corte, V.; Catillon, M.; Bruyneel, E.; Lentz, D.; Plastino, J.; Gettemans, J.; Friederich, E. (**2006**) Phosphorylation on Ser5 increases the F-actin-binding activity of L-plastin and promotes its targeting to sites of actin assembly in cells. *J. Cell Sci.*, 119(Pt 9), 1947-1960.

Kierzek, A.M.; Zaim, J.; Zielenkiewicz, P. (**2001**) The effect of transcription and translation initiation frequencies on the stochastic fluctuations in prokaryotic gene expression. *J. Biol. Chem.*, 276(11), 8165-8172.

Kouyama, T.; Mihashi, K. (**1981**) Fluorimetry study of N-(1-pyrenyl)iodoacetamide-labelled F-actin. Local structural change of actin protomer both on polymerization and on binding of heavy meromyosin. *Eur J Biochem*, 114(1), 33-38.

Kovar, D.R. (**2006**) Molecular details of formin-mediated actin assembly. *Curr. Opin. Cell Biol.*, 18(1), 11-17.

Li, G.; Tang, J. (**2004**) Diffusion of actin filaments within a thin layer between two walls. *Phys. Rev. E*, 69(6), 61921.

Loomis, P.A.; Zheng, L.; Sekerkova, G.; Changyaleket, B.; Mugnaini, E.; Bartles, J.R. (**2003**) Espin cross-links cause the elongation of microvillus-type parallel actin bundles in vivo. *J. Cell Biol.*, 163(5), 1045-1055.

Mahaffy, R.E.; Pollard, T.D. (**2006**) Kinetics of the formation and dissociation of actin filament branches mediated by Arp2/3 complex. *Biophys. J.*, 91(9), 3519-3528.

Marcy, Y.; Prost, J.; Carlier, M.F.; Sykes, C. (**2004**) Forces generated during actin-based propulsion: a direct measurement by micromanipulation. *Proc. Natl. Acad. Sci. USA*, 101(16), 5992-5997.

McAdams, H.H.; Shapiro, L. (**1995**) Circuit simulation of genetic networks. *Science*, 269(5224), 650-656.

McGrath, J.L.; Osborn, E.A.; Tardy, Y.S.; Dewey, C.F., Jr.; Hartwig, J.H. (**2000**) Regulation of the actin cycle in vivo by actin filament severing. *Proc. Natl. Acad. Sci. USA*, 97(12), 6532-6537.

Melki, R.; Fievez, S.; Carlier, M.F. (**1996**) Continuous monitoring of Pi release following nucleotide hydrolysis in actin or tubulin assembly using 2-amino-6-mercapto-7-methylpurine ribonucleoside and purinenucleoside phosphorylase as an enzyme-linked assay. *Biochemistry*, 35, 12038-12045.

Ming, D.; Kong, Y.; Wu, Y.; Ma, J. (**2003**) Simulation of F-actin filaments of several microns. *Biophys. J.*, 85(1), 27-35.

Mogilner, A.; Edelstein-Keshet, L. (**2002**) Regulation of actin dynamics in rapidly moving cells: a quantitative analysis. *Biophys. J.*, 83(3), 1237-1258.

Mogilner, A.; Oster, G. (**2003**) Force generation by actin polymerization II: the elastic ratchet and tethered filaments. *Biophys. J.*, 84(3), 1591-1605.

Mogilner, A.; Rubinstein, B. (**2005**) The physics of filopodial protrusion. *Biophys. J.*, 89(2), 782-795.

Nazarov, P.V.; Apanasovich, V.V.; Lutkovski, V.M.; Yatskou, M.M.; Koehorst, R.B.; Hemminga, M.A. (**2004**) Artificial neural network modification of simulation-based fitting: application to a protein-lipid system. *J. Chem. Inf. Comput. Sci.*, 44(2), 568-574.

Nazarov, P.V.; Koehorst, R.B.; Vos, W.L.; Apanasovich, V.V.; Hemminga, M.A. (**2006**) FRET study of membrane proteins: simulation-based fitting for analysis of membrane protein embedment and association. *Biophys. J.*, 91(2), 454-466.

Noireaux, V.; Golsteyn, R.M.; Friederich, E.; Prost, J.; Antony, C.; Louvard, D.; Sykes, C. (**2000**) Growing an actin gel on spherical surfaces. *Biophys. J.*, 78(3), 1643-1654.

Plastino, J.; Olivier, S.; Sykes, C. (**2004**) Actin filaments align into hollow comets for rapid VASP-mediated propulsion. *Curr. Biol.*, 14(19), 1766-1771.

Pollard, T.D. (**1986**) Rate constants for the reactions of ATP- and ADP-actin with the ends of actin filaments. *J. Cell Biol.*, 103, 2747-2754.

Pollard, T.D.; Beltzner, C.C. (**2002**) Structure and function of the Arp2/3 complex. *Curr. Opin. Struct. Biol.*, 12(6), 768-774.

Pollard, T.D.; Borisy, G.G. (**2003**) Cellular motility driven by assembly and disassembly of actin filaments. *Cell*, 112(4), 453-465.

Puchalka, J.; Kierzek, A.M. (**2004**) Bridging the gap between stochastic and deterministic regimes in the kinetic simulations of the biochemical reaction networks. *Biophys. J.*, 86(3), 1357-1372.

Romero, S.; Le Clainche, C.; Didry, D.; Egile, C.; Pantaloni, D.; Carlier, M.F. (**2004**) Formin is a processive motor that requires profilin to accelerate actin assembly and associated ATP hydrolysis. *Cell*, 119(3), 419-429.

Samarin, S.; Romero, S.; Kocks, C.; Didry, D.; Pantaloni, D.; Carlier, M.F. (**2003**) How VASP enhances actin-based motility. *J. Cell Biol.*, 163(1), 131-142.

Schafer, D.; Jennings, P.; Cooper, J. (**1996**) Dynamics of capping protein and actin assembly in vitro: Uncapping barbed ends by polyphosphoinisitides. *J. Cell Biol.*, 135, 169-179.

Sept, D.; McCammon, J.A. (**2001**) Thermodynamics and kinetics of actin filament nucleation. *Biophys. J.*, 81(2), 667-674.

Sirotkin, V.; Beltzner, C.C.; Marchand, J.B.; Pollard, T.D. (**2005**) Interactions of WASp, myosin-I, and verprolin with Arp2/3 complex during actin patch assembly in fission yeast. *J. Cell Biol.*, 170(4), 637-648.

Soo, F.S.; Theriot, J.A. (**2005**) Large-scale quantitative analysis of sources of variation in the actin polymerization-based movement of Listeria monocytogenes. *Biophys. J.*, 89(1), 703-723.

Tracqui, P.; Promayon, E.; Amar, P.; Huc, N.; Norris, V.; Martiel, J.L. (**2004**) Emergent features of cell structural dynamics: a review of models based on tensegrity and nonlinear oscillations.

Tseng, Y.; Schafer, B.W.; Almo, S.C.; Wirtz, D. (**2002**) Functional synergy of actin filament cross-linking proteins. *J. Biol. Chem.*, 277(28), 25609-25616.

Upadhyaya, A.; Chabot, J.R.; Andreeva, A.; Samadani, A.; van Oudenaarden, A. (**2003**) Probing polymerization forces by using actin-propelled lipid vesicles. *Proc. Natl. Acad. Sci. USA*, 100(8), 4521-4526.

van der Gucht, J.; Paluch, E.; Plastino, J.; Sykes, C. (**2005**) Stress release drives symmetry breaking for actin-based movement. *Proc. Natl. Acad. Sci. USA*, 102(22), 7847-7852.

van Oudenaarden, A.; Theriot, J.A. (**1999**) Cooperative symmetry-breaking by actin polymerization in a model for cell motility. *Nat. Cell Biol.*, 1(8), 493-499.

Vignjevic, D.; Yarar, D.; Welch, M.D.; Peloquin, J.; Svitkina, T.; Borisy, G.G. (**2003**) Formation of filopodia-like bundles in vitro from a dendritic network. *J. Cell Biol.*, 160(6), 951-962.

Vilar, J.M.; Kueh, H.Y.; Barkai, N.; Leibler, S. (**2002**) Mechanisms of noise-resistance in genetic oscillators. *Proc. Natl. Acad. Sci. U.S.A.*, 99(9), 5988-5992.

Yamazaki, D.; Kurisu, S.; Takenawa, T. (**2005**) Regulation of cancer cell motility through actin reorganization. *Cancer Sci.*, 96(7), 379-386.

Yatskou, M.M.; Donker, H.; Novikov, E.G.; Koehorst, R.B.M.; van Hoek, A.; Apanasovich, V.V.; Schaafsma, T.J. (**2001**) Nonisotropic excitation energy transport in organized molecular systems: Monte Carlo simulation-based analysis of time-resolved fluorescence. *J. Phys. Chem. A*, 105(41), 9498-9508.

Zicha, D.; Dobbie, I.M.; Holt, M.R.; Monypenny, J.; Soong, D.Y.; Gray, C.; Dunn, G.A. (**2003**) Rapid actin transport during cell protrusion. *Science*, 300(5616), 142-145.